Evolutionary transcriptomics implicates *HAND2* in the origins of implantation and regulation of gestation length

Mirna Marinić[1†], Katelyn Mika[1†], Sravanthi Chigurupati[1‡], Vincent J Lynch[2*]

[1]Department of Human Genetics, University of Chicago, Chicago, United States; [2]Department of Biological Sciences, University at Buffalo, Buffalo, United States

Abstract The developmental origins and evolutionary histories of cell types, tissues, and organs contribute to the ways in which their dysfunction produces disease. In mammals, the nature, development and evolution of maternal-fetal interactions likely influence diseases of pregnancy. Here we show genes that evolved expression at the maternal-fetal interface in Eutherian mammals play essential roles in the evolution of pregnancy and are associated with immunological disorders and preterm birth. Among these genes is *HAND2*, a transcription factor that suppresses estrogen signaling, a Eutherian innovation allowing blastocyst implantation. We found dynamic *HAND2* expression in the decidua throughout the menstrual cycle and pregnancy, gradually decreasing to a low at term. HAND2 regulates a distinct set of genes in endometrial stromal fibroblasts including *IL15*, a cytokine also exhibiting dynamic expression throughout the menstrual cycle and gestation, promoting migration of natural killer cells and extravillous cytotrophoblasts. We demonstrate that *HAND2* promoter loops to an enhancer containing SNPs implicated in birth weight and gestation length regulation. Collectively, these data connect *HAND2* expression at the maternal-fetal interface with evolution of implantation and gestational regulation, and preterm birth.

*For correspondence:
vjlynch@buffalo.edu

Present address: [†]Department of Organismal Biology and Anatomy, University of Chicago, Chicago, United States; [‡] AbbVie, North Chicago, United States

Introduction

The ontogeny and evolutionary history of cell types, tissues, and organ systems, as well as the life histories of organisms bias the ways in which dysfunctions in those systems underlie disease (*Varki, 2012*). Thus, a mechanistic understanding of how cells, tissues, and organs evolved their functions, and how organism's life histories influence them, may provide clues to the molecular etiologies of disease. The most common way of utilizing evolutionary information to characterize the genetic architecture of disease is to link genetic variation within a species to phenotypes using quantitative trait loci (QTL) or genome-wide association studies (GWAS). An alternative approach is to identify fixed genetic differences between species that are phylogenetically correlated with different disease relevant phenotypes. While the risk of cancer increases with the age of an individual, for example, the prevalence of cancer types varies by species (*Abegglen et al., 2015*), likely because of differences in genetic susceptibility to specific cancers, structure of organ and tissue systems, and life exposures to carcinogens (*Varki and Varki, 2015*). Similarly, the risk of cardiovascular disease (CVD) increases with age across species, but the pathophysiology of CVD can differ even between closely related taxa such as humans, in which CVD predominantly results from coronary artery atherosclerosis, and the other Great Apes (Hominids), in which CVD is most often associated with interstitial myocardial fibrosis (*Varki et al., 2009*).

Extant mammals span major stages in the origins and diversification of pregnancy, thus a mechanistic understanding of how pregnancy originated and diverged may provide unique insights into the ontogenetic origins of pregnancy disorders. The platypus and echidna (Monotremes) are oviparous, but the embryo is retained in the uterus for 10–22 days, during which the developing fetus is

nourished by maternal secretions delivered through a simple placenta, prior to the laying of a thin, poorly mineralized egg that hatches in ~2 weeks (*Hill, 1936*). Live birth (viviparity) evolved in the stem-lineage of Therian mammals, but Marsupials and Eutherian ('Placental') mammals have dramatically different reproductive strategies. In Marsupials, pregnancies are generally short (~25 days) and completed within the span of a single estrous cycle (*Renfree and Shaw, 2001*; *Renfree, 2010*). Eutherians, in contrast, evolved a suite of traits that support prolonged pregnancies (up to 670 days in African elephant), including an interrupted estrous cycle, which allows for gestation lengths longer than a single reproductive cycle, maternal-fetal communication, maternal recognition of pregnancy, implantation of the blastocyst and placenta into uterine tissue, differentiation (decidualization) of endometrial stromal fibroblasts (ESFs) in the uterine lining into decidual stromal cells (DSCs), and maternal immunotolerance of the antigenically distinct fetus, that is the fetal allograft (*Guleria and Pollard, 2000*; *Moffett and Loke, 2004*; *Erlebacher, 2013*).

Gene expression changes at the maternal-fetal interface underlie evolutionary differences in pregnancy (*Hou et al., 2012*; *Lynch et al., 2015*; *Armstrong et al., 2017*), and thus likely also pathologies of pregnancy such as infertility, recurrent spontaneous abortion (*Kosova et al., 2015*), preeclampsia (*Elliot, 2017*; *Arthur, 2018*; *Varas Enriquez et al., 2018*), and preterm birth (*Plunkett et al., 2011*; *Swaggart et al., 2015*; *LaBella, 2019*). Here, we assembled a collection of gene expression data from the pregnant/gravid maternal-fetal interface of tetrapods and used evolutionary methods to reconstruct gene expression changes during the origins of mammalian pregnancy. We found that genes that evolved to be expressed at the maternal-fetal interface in the Eutherian stem-lineage were enriched for immune functions and diseases, as well as preterm birth. Among the recruited genes was the transcription factor *Heart- and neural crest derivatives-expressed protein 2* (*HAND2*), which plays essential roles in neural crest development (*Srivastava et al., 1997*), cardiac morphogenesis (*Srivastava et al., 1997*; *Shen et al., 2010*; *Tamura et al., 2013*; *Lu et al., 2016*; *Sun et al., 2016*), and suppressing estrogen signaling during the period of uterine receptivity to implantation (*Huyen and Bany, 2011*; *Li et al., 2011*; *Shindoh et al., 2014*; *Fukuda et al., 2015*; *Mestre-Citrinovitz et al., 2015*; *Murata et al., 2019*; *Šućurović et al., 2020*). We determined that *HAND2* expression at the first trimester maternal-fetal interface was almost entirely restricted to cell types in ESF lineage and is regulated by multiple transcription factors that control progesterone responsiveness. Moreover, the *HAND2* promoter loops to an enhancer with single-nucleotide polymorphisms (SNPs) that have been implicated by GWAS in the regulation of gestation length (*Warrington et al., 2019*; *Sakabe et al., 2020*). Furthermore, we showed that HAND2 regulates interleukin 15 (*IL15*) expression in ESFs, and that ESF-derived IL15 influences the migration of natural killer and trophoblast cells. These data suggest that HAND2 and IL15 signaling played an important role in the evolution of implantation and regulation of gestation length.

Results

Genes that evolved endometrial expression in Eutherian mammals are enriched in immune functions

We previously used comparative transcriptomics to reconstruct the evolution of gene expression at the maternal-fetal interface during the origins of mammalian pregnancy (*Lynch et al., 2015*). Here, we assembled a collection of new and existing transcriptomes from the pregnant/gravid endometria of 15 Eutherian mammals, 3 Marsupials, 1 Monotreme (platypus), 2 birds, 5 lizards, and 1 amphibian (*Figure 1A* and *Figure 1—source data 1*). The complete dataset includes expression information for 21,750 genes from 27 species. Next, we transformed continuous transcript abundance estimates values into discrete character states such that genes with Transcripts Per Million (TPM) $\geq$ 2.0 were coded as expressed (state = 1), genes with TPM < 2.0 were coded as not expressed (state = 0), and genes without data in specific species were coded as missing (state = ?). We then used parsimony to reconstruct ancestral transcriptomes and trace the evolution of gene expression gains (0 $\rightarrow$ 1) and losses (1 $\rightarrow$ 0) in the endometrium (*Figure 1—source data 2*).

We identified 958 genes that most parsimoniously evolved endometrial expression in the Eutherian stem-lineage, including 149 that unambiguously evolved endometrial expression (*Figure 1A* and *Figure 1—source data 3*). These 149 genes were significantly enriched in pathways related to
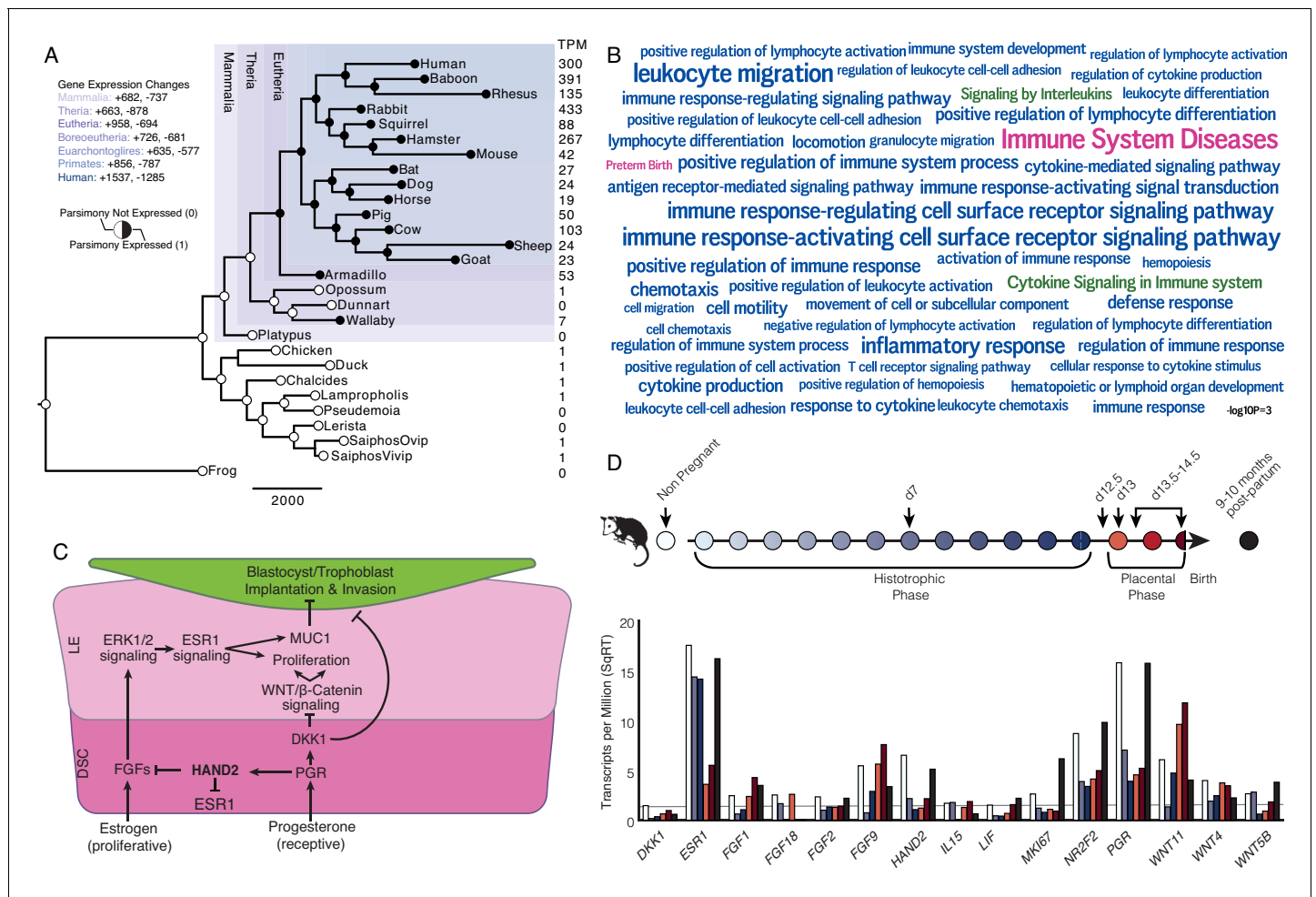
Figure 1. Recruitment of HAND2-mediated anti-estrogenic signaling in the Eutherian endometrium. (A) Evolution of *HAND2* expression at the maternal-fetal interface. Amniotes phylogeny with horizontal branch lengths drawn proportional to the number of gene expression changes inferred by parsimony (most parsimonious reconstruction). Circles indicate *HAND2* expression in extant species and ancestral reconstructions. Black, expressed (state = 1). White, not expressed (state = 0). Inset legend shows the number of most gene expression changes from the root node to human (+ = gene expression gained; - = gene expression lost). Numbers to the right indicate *HAND2* expression in TPM for each respective species. (B) WordCloud of biological pathways (green), human disease phenotypes (pink), and biological process gene ontology terms (blue) enriched among 149 unambiguously recruited genes in the Eutherian stem-lineage. Term size is shown scaled to -log10 p-value (see inset scale). (C) Cartoon model of estrogen signaling and HAND2-mediated anti-estrogenic signaling in the endometrium. The estrogen-mediated signaling network is suppressed by progesterone through the activation of HAND2 and antagonists of canonical WNT/β-catenin-mediated signaling pathways such as DKK1. In the proliferative phase of the reproductive cycle, estrogen acts through ESR1 in stromal cells to increase the production of fibroblast growth factors (FGFs), which serve as paracrine signals leading to sustained proliferation of epithelial cells. Active estrogen signaling maintains epithelial expression of Mucin 1 (MUC1), a cell surface glycoprotein that acts as a barrier to implantation. During the receptive phase of the cycle, however, progesterone induces HAND2 and DKK1 expression in the endometrial stroma, inhibiting production of FGFs, suppressing epithelial proliferation and antagonizing estrogen-mediated expression of MUC1, thereby promoting uterine receptivity to implantation. DSC = decidual stromal cells, LE = luminal epithelium. (D) Gene expression time course through opossum pregnancy. Upper, schematic of gestation length in *Monodelphis domestica* in which the histotrophic phase lasts from day 1 to day 12, hatching occurs on day 12.5, the placental phase lasts from day 13 to day 14.5, and birth occurs on day 14.5. Lower, data shown as square root (SqRT) transformed TPM. The TPM = 2 expression cutoff is shown as a horizontal gray line. *M. domestica* RNA-Seq data from ***Lynch et al., 2015***; ***Hansen et al., 2016***; ***Griffith et al., 2017***; ***Griffith et al., 2019***.

The online version of this article includes the following source data and figure supplement(s) for figure 1:

Source data 1. Species and gene expression information.

Source data 2. Binary encoded endometrial gene expression dataset.

Source data 3. Genes (HUGO gene names) that unambiguously evolved endometrial expression in the Eutherian stem-lineage ('Recruited Genes').

Source data 4. Top 100 pathways (Wikipathway, Reactome, KEGG) in which Eutherian recruited genes are enriched.

Source data 5. Top 100 human phenotype (disease) ontology terms in which Eutherian recruited genes are enriched.

Source data 6. Top 100 biological process gene ontology (GO) terms in which Eutherian recruited genes are enriched.

Figure 1 continued on next page

Figure 1 continued

Source data 7. RNA-Seq data from opossum endometrial samples.

Source data 8. Database of genes implicated in preterm birth.

Figure supplement 1. The unpaired mean difference in *HAND2* expression between non-Gravid and Gravid wallaby samples is −8.6 [95.0% CI: −10.7 – −6.46].

Figure supplement 1—source data 1. Uterine gene expression data (in TPM) from four Gravid (orange - Wal38, Wal40, Wal57, and Wal59) and four non-Gravid (blue - Wal39, Wal41, Wal58, and Wal60) tammar wallabies.

Figure supplement 2. Immunohistochemistry showing phosphorylated ESR1 (pESR1), phosphorylated MAPK1/2 (pERK1/2) and MUC1 expression in paraffin-embedded 12.5d pregnant *Monodelphis domestica* endometrium compared to control (IgG).

the immune system (*Figure 1B* and *Figure 1—source data 4–6*), although only two pathways were enriched at False Discovery Rate (FDR) ≤ 0.10, namely, 'Cytokine Signaling in Immune System' (hypergeometric p = 1.97×10^{-5}, FDR = 0.054) and 'Signaling by Interleukins' (hypergeometric p = 4.09×10^{-5}, FDR = 0.067). Unambiguously recruited genes were also enriched in numerous human phenotype ontology terms but only two, 'Immune System Diseases' (hypergeometric p = 3.15×10^{-8}, FDR = 2.52×10^{-4}) and 'Preterm Birth' (hypergeometric p = 4.04×10^{-4}, FDR = 8.07×10^{-4}), were enriched at FDR ≤ 0.10. In contrast, these genes were enriched in numerous biological process gene ontology (GO) terms at FDR ≤ 0.10, nearly all of which were related to regulation of immune system, including 'Leukocyte Migration' (hypergeometric p = 1.17×10^{-7}, FDR = 1.29×10^{-3}), 'Inflammatory Response' (hypergeometric p = 8.07×10^{-7}, FDR = 2.21×10^{-3}), and 'Cytokine-mediated Signaling Pathway' (hypergeometric p = 2.18×10^{-5}, FDR = 0.013).

Recruitment of *HAND2* and anti-estrogenic signaling in Eutherians

Among the genes that unambiguously evolved endometrial expression in the Eutherian stem-lineage was the basic helix-loop-helix family transcription factor *Heart- and neural crest derivatives-expressed protein 2* (*HAND2*). *HAND2* plays an essential role in mediating the anti-estrogenic action of progesterone and the establishment of uterine receptivity to implantation (*Figure 1C*; *Huyen and Bany, 2011*; *Li et al., 2011*; *Fukuda et al., 2015*; *Mestre-Citrinovitz et al., 2015*), suggesting that the silencing of estrogen signaling during the window of implantation is a derived trait in Eutherian mammals. Notably, this silencing is not observed in the pregnant endometrium of Marsupials such as the brush-tailed possum (*Trichosurus vulpecula*) (*Young and McDonald, 1982*; *Curlewis and Stone, 1987*) and tammar wallaby (*Macropus eugenii*) (*Renfree and Blanden, 2000*).

To investigate further, we used the short-tailed opossum (*Monodelphis domestica*) as a model of pregnancy in Marsupials. *M. domestica* lacks implantation and thus is a good representative of pregnancy in the Therian common ancestor, in contrast to other Marsupials, such as the tammar wallaby, which have derived traits such as delayed ovulation, independently evolved maternal recognition of pregnancy and expression of *HAND2* at low levels during gravidity (*Figure 1A* and *Figure 1—figure supplement 1—source data 1*, *Figure 1—figure supplement 1*). Using existing RNA-Seq data from short-tailed opossum endometria, we analyzed a time course consisting of day 7 (during the histotrophic phase), day 12.5 (just after hatching and during the transition from the histotrophic to the placental phase), day 13 (early placental phase), day 13.5–14.5 (during the late placental to early parturition phase), and 9–10 month post-partum, as well as non-pregnant control (*Figure 1D*; *Lynch et al., 2015*; *Hansen et al., 2016*; *Griffith et al., 2017*; *Griffith et al., 2019*). We found that *HAND2* was abundantly expressed in the non-pregnant endometrium and down-regulated throughout the histotrophic phase, reaching a low (TPM < 2) at 12.5d, and subsequently increasing in expression in the 13.5-14d samples near term. *ESR1*, *FGF2*, *FGF9*, *FGF18* and several *WNT* genes that stimulate proliferation of the luminal epithelia were abundantly expressed (*Figure 1D* and *Figure 1—source data 7*), consistent with persistent estrogen signaling during pregnancy (*Renfree and Blanden, 2000*). Both *HAND2* and *ESR1* decrease during gestation (*Figure 1D*), suggesting that the inhibition of estrogen signaling by *HAND2* seen in Eutherians does not occur in opossum endometrium – if it did, one would expect *ESR1* expression to increase as *HAND2* expression decreased. Similarly, *HAND2* is down-regulated during pregnancy in the tammar wallaby (*Figure 1—figure supplement 1—source data 1*, *Figure 1—figure supplement 1*). Immunohistochemistry (IHC) on opossum endometrial sections from day 12.5 pregnant endometrium stained strongly for estrogen receptor alpha (*ESR1*; ERα) phosphorylated at serine 118, a mark of transcriptionally active ERα

(*Kato et al., 1995*), as well as phosphorylated ERK1/2, and MUC1 (*Figure 1—figure supplement 2*), which is also consistent with active estrogen signaling.

HAND2 is expressed in endometrial stromal fibroblast lineage cells

To determine which cell types at the human maternal-fetal interface express *HAND2*, we used previously generated single-cell RNA-Seq (scRNA-Seq) data from the first trimester decidua (*Vento-Tormo et al., 2018*). *HAND2* expression was almost entirely restricted to cell populations in the endometrial stromal fibroblast lineage (see Materials and methods for cell type naming convention), with particularly high expression in ESF2s and DSCs (*Figure 2A*). Interestingly, while it is generally thought that ESFs are not present in the pregnant endometrium, previous studies have demonstrated that ESFs retain a presence in the endometrium from the first trimester all the way to term (*Richards et al., 1995*; *Suryawanshi et al., 2018*; *Muñoz-Fernández et al., 2019*; *Sakabe et al., 2020*).

HAND2 protein was localized to nuclei in ESF lineage cells in human pregnant decidua (*Figure 2B*) from Human Protein Atlas IHC data (*Uhlén et al., 2015*). We also used existing functional genomics data to explore the regulatory status of the *HAND2* locus (see Materials and methods for references). Consistent with active expression, the *HAND2* locus in human DSCs is marked by histone modifications that typify enhancers (H3K27ac) and promoters (H3K4me3) and is located in a region of open chromatin as assessed by ATAC-, DNaseI- and FAIRE-Seq. Additionally, it is bound by transcription factors that establish endometrial stromal cell type identity and mediate decidualization, including the progesterone receptor (PGR), NR2F2 (COUP-TFII), GATA2, FOSL2, FOXO1, as well as polymerase II (*Figure 2C*). The *HAND2* promoter loops to several distal enhancers, as assessed by H3K27ac HiChIP data generated from a normal hTERT-immortalized endometrial cell line (E6E7hTERT), including a region bound by PGR, NR2F2, GATA2, FOSL2, and FOXO1, that also contains SNPs associated with gestation length in recent GWAS (*Warrington et al., 2019*; *Sakabe et al., 2020*; *Figure 2C*). *HAND2* was significantly upregulated by decidualization of human ESFs into DSCs by cAMP/progesterone treatment (Log_2FC = 1.28, p = 2.62×10^{-26}, FDR = 1.16×10^{-24}), and significantly downregulated by siRNAs targeting PGR (Log_2FC = −0.90, p = 7.05×10^{-15}, FDR = 2.03×10^{-13}) and GATA2 (Log_2FC = −2.73, p = 0.01, FDR = 0.19) (*Figure 2D*). In contrast, siRNA-mediated knockdown of neither NR2F2 (Log_2FC = −0.91, p = 0.05, FDR = 1.0) nor FOXO1 (Log_2FC = 0.08, p = 0.49, FDR = 0.74) significantly altered *HAND2* expression (*Figure 2D* and see Materials and methods for references).

Differential *HAND2* expression throughout the menstrual cycle and pregnancy

Our observation that *HAND2* is progesterone responsive suggests it may be differentially expressed throughout the menstrual cycle and pregnancy. To explore this possibility, we utilized previously published gene expression datasets generated from the endometrium across the menstrual cycle (*Talbi et al., 2006*) and from the basal plate from mid-gestation to term (*Winn et al., 2007*). *HAND2* expression tended to increase from proliferative through the early and middle secretory phases, reaching a peak in the late secretory phase of the menstrual cycle (*Figure 2E*). In stark contrast, *HAND2* decreases in expression from the first trimester to term (*Figure 2F*). For comparison, 9% of genes were down-regulated between weeks 14–19 and 37–40 of pregnancy (FDR ≤ 0.10). We also used previously published gene expression datasets to explore if *HAND2* was associated with disorders of pregnancy (*Lédée et al., 2011*; *Garrido-Gomez et al., 2017*). Although sample sizes of these datasets are small, and the intrinsic temporo-spatial heterogeneity of the endometrium remains a potential confounding factor, we found that *HAND2* was dysregulated in the endometria of women with implantation failure (IF) and recurrent spontaneous abortion (RSA), while it was not differentially expressed in ESFs or DSCs from women with preeclampsia (PE), compared to controls (*Figure 2G*).

HAND2 regulates a distinct set of target genes

HAND2 expression has previously been shown to play a role in orchestrating the transcriptional response to progesterone during decidualization in human and mouse DSCs (*Huyen and Bany, 2011*; *Li et al., 2011*; *McConaha et al., 2011*; *Shindoh et al., 2014*; *Murata et al., 2020*). However,
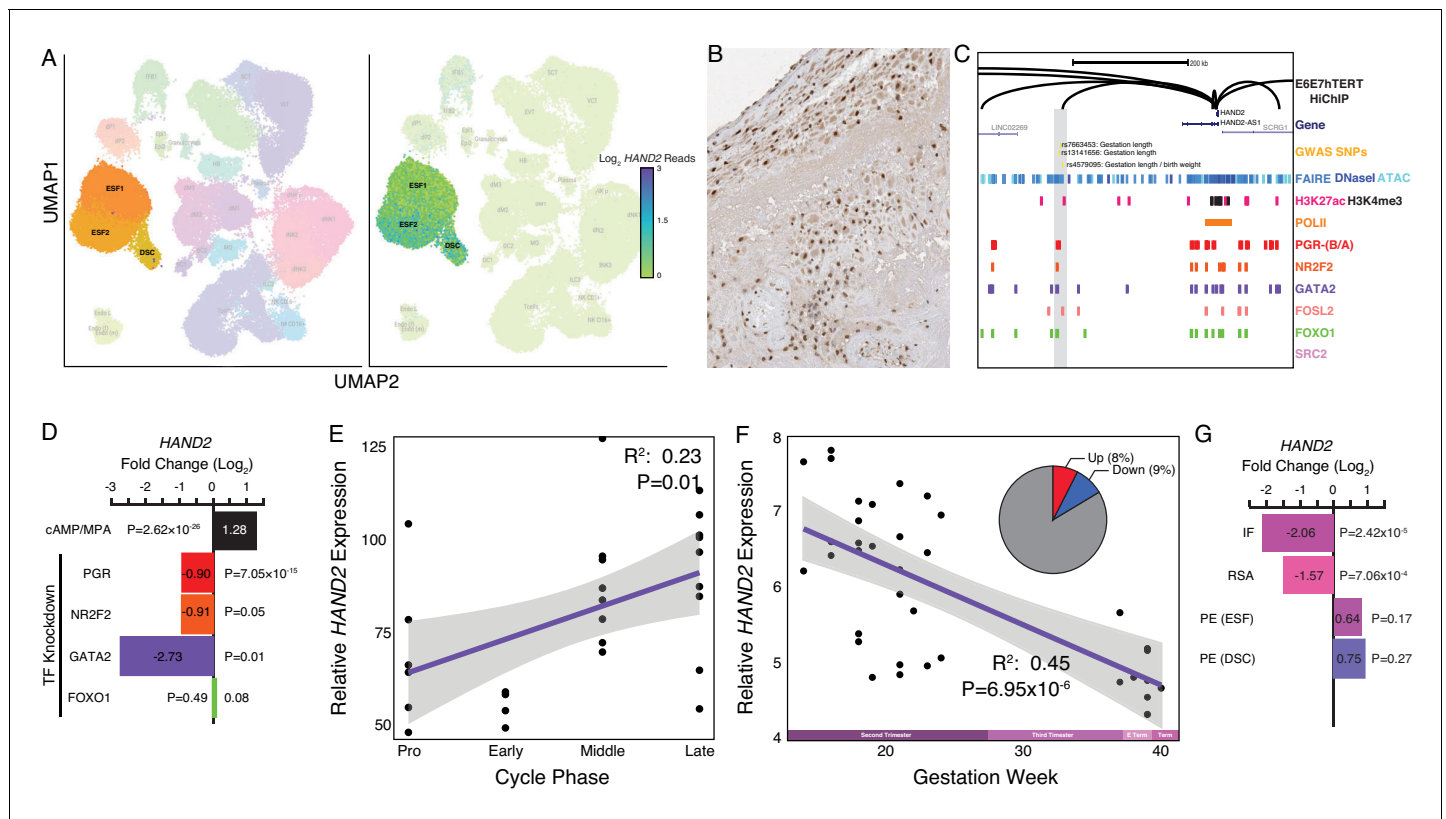
Figure 2. Expression of *HAND2* at the maternal-fetal interface. (**A**) UMAP clustering of scRNA-Seq data from human first trimester maternal-fetal interface. Left, clusters colored according to inferred cell type. The ESF1, ESF2, and DSC clusters are highlighted. Right, cells within clusters are colored according to *HAND2* expression level. scRNA-Seq data from *Vento-Tormo et al., 2018*. (**B**) HAND2 protein expression in human pregnant decidua, with strong staining and localization in the nuclei of endometrial stromal cells. Image credit: Human Protein Atlas. (**C**) Regulatory landscape of the *HAND2* locus. Chromatin loops inferred from H3K27ac HiChIP, regions of open chromatin inferred from FAIRE-, DNaseI, and ATAC-Seq, and the locations of histone modifications and transcription factor ChIP-Seq peaks are shown. The location of SNPs associated with gestation length / birth weight is also shown (highlighted in gray). Note that the *HAND2* promoter forms a long-range loop to a region marked by H3K27ac and bound by PGR, NR2F2 (COUP-TFII), GATA2, FOSL2, and FOXO1. (**D**) *HAND2* expression is up-regulated by *in vitro* decidualization of ESFs into DSC by cAMP/ progesterone treatment, and down-regulated by siRNA-mediated knockdown of PGR and GATA2, but not NR2F2 or FOXO1. n = 3 per transcription factor knockdown. (**E**) Relative expression of *HAND2* in the proliferative (n = 6), early (n = 4), middle (n = 9), and late (n = 8) secretory phases of the menstrual cycle. Note that outliers are excluded from the figure but not the regression; 95% CI is shown in gray. Gene expression data from *Talbi et al., 2006*. (**F**) Relative expression of *HAND2* in the basal plate from mid-gestation to term (14–40 weeks, n = 36); 95% CI is shown in gray. Inset, percent of up- (Up) and down-regulated (Down) genes between weeks 14–19 and 37–40 of pregnancy (FDR $\leq$ 0.10). Gene expression data from *Winn et al., 2007*. (**G**) *HAND2* expression is significantly down-regulated in the endometria of women with implantation failure (IF, n = 5) and recurrent spontaneous abortion (RSA, n = 5) compared to fertile controls (n = 5), but is not differentially expressed in ESFs or DSCs from women with preeclampsia (PE, n = 5) compared to healthy controls (n = 5). Gene expression data for RSA and IF from *Lédée et al., 2011* and for PE from *Garrido-Gomez et al., 2017*.

whether *HAND2* has functions in other endometrial stromal lineage cells such as ESFs, which persist in the pregnant endometrium till term (*Richards et al., 1995*; *Suryawanshi et al., 2018*; *Muñoz-Fernández et al., 2019*; *Sakabe et al., 2020*) but have received less attention than DSCs during pregnancy, is unknown. Therefore, we used siRNA to knockdown *HAND2* expression in human hTERT-immortalized ESFs (T-HESC) and assayed global gene expression changes by RNA-Seq 48 hr after knockdown. We found that *HAND2* was knocked down ~78% (p = 7.79×10^{-3}) by siRNA treatment (*Figure 3A*), which dysregulated the expression of 553 transcripts (489 genes) at FDR $\leq$ 0.10 (*Figure 3A* and *Figure 3—source data 1*). Genes dysregulated by *HAND2* knockdown were enriched in several pathways and human phenotype ontologies relevant to endometrial stromal cells and pregnancy in general (*Figure 3B* and *Figure 3—source data 2, 3*).
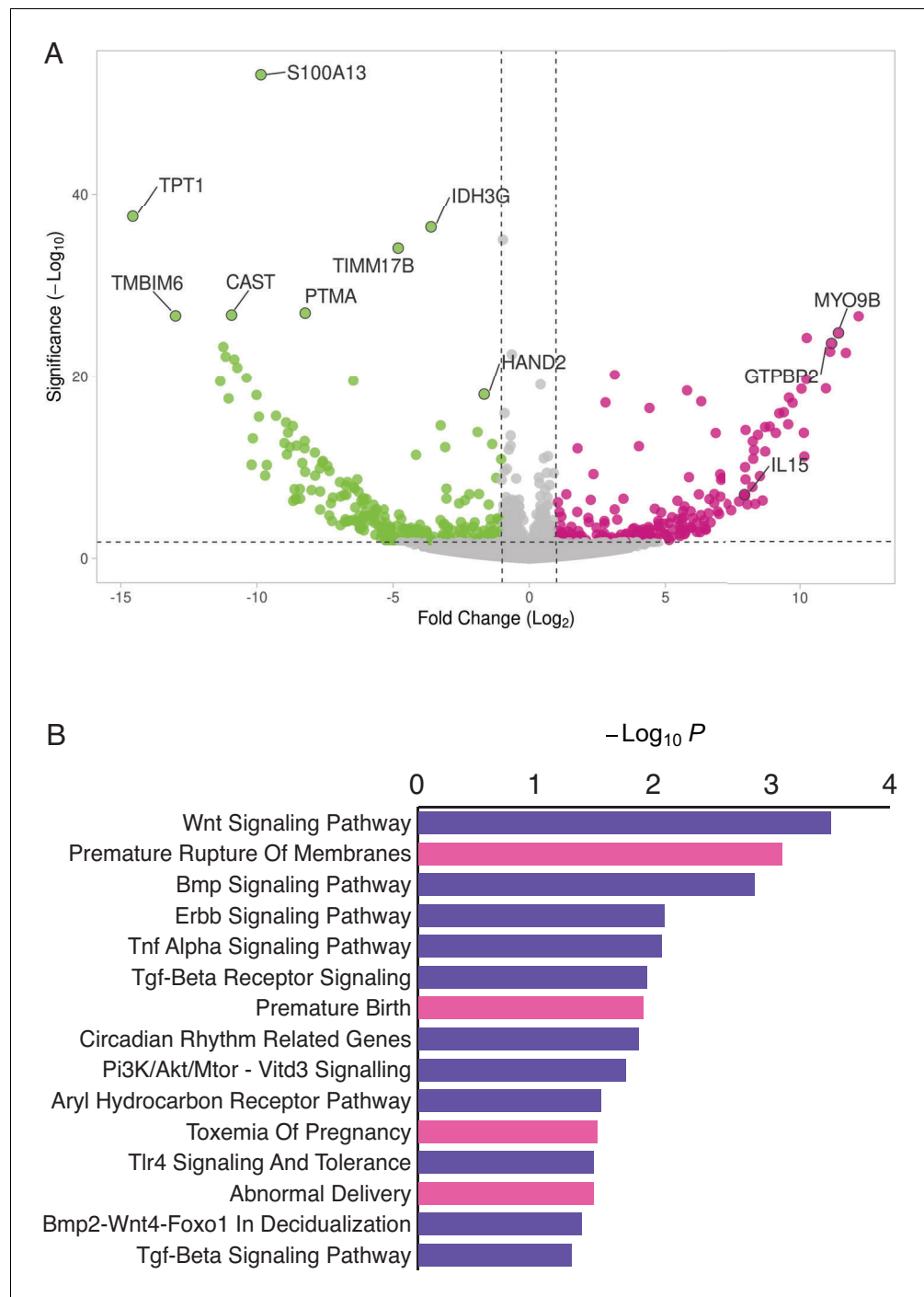
Figure 3. HAND2 regulates a distinct set of target genes, including *IL15*. (**A**) Volcano plot of gene expression upon *HAND2* knockdown. Only genes that are significantly differentially expressed (DE) with FDR ≤ 0.10 are colored. Genes with ≥ 1 fold changes in expression are shown in pink (up-regulated), green (down-regulated) or gray (not differentially expressed). X-axis shows $\log_2$ fold change, Y-axis shows Wald statistic p-value, horizontal dashed line indicates FDR = 0.10. Full list of DE genes can be found in *Figure 3—source data 1*. (**B**) Pathways (purple) and human phenotype ontologies (pink) in which genes dysregulated upon *HAND2* knockdown are enriched. We used a hypergeometric p-value to determine enriched pathway and disease ontology terms. The Benjamini-Hochburg Adjusted p-value (FDR), Odds Ratio, Combined Score, and Genes associated with each term can be found in *Figure 3—source data 2* and *Figure 3—source data 3*.

The online version of this article includes the following source data for figure 3:

Source data 1. Genes differentially expressed (DE) upon *HAND2* knockdown.

Source data 2. Pathways (Wikipathway 2019) enriched among genes differentially expressed by *HAND2* knockdown.

Source data 3. Human phenotype (disease) ontology terms enriched among genes differentially expressed by *HAND2* knockdown.

Enriched pathways play a role in decidualization (e.g. 'Wnt Signaling', 'BMP Signaling', 'ErbB Signaling', 'TGF-beta Receptor Signaling' and 'BMP2-WNT4-FOXO1 Pathway in Human Primary Endometrial Stromal Cell Differentiation'), as well as in placental bed development disorders and preeclampsia, the induction of pro-inflammatory factors via nuclear factor-κB (NFκB), mediation of maternal immunotolerance to the fetal allograft, circadian rhythm in association with implantation and parturition, and the decidual inflammation, senescence, and parturition. Selected pathways and associated references are listed in *Table 1*.

Enriched human phenotype ontology terms were related to complications of pregnancy, including 'Premature Rupture of Membranes', 'Premature Birth', 'Toxemia of Pregnancy' (preeclampsia) and 'Abnormal Delivery'. We also observed that several genes in the NFκB pathway, such as MYD88, CHUK, IκBKE, NFκBIE, and RTKN2 were differentially expressed; NFκB signaling has been associated with the molecular etiology of preterm birth (*Allport et al., 2001*; *Lindström and Bennett, 2005*).

HAND2 regulates *IL15* expression in endometrial stromal fibroblast lineage cells

Among the genes dysregulated by *HAND2* knockdown in ESFs was *IL15* (Log$_2$FC = 7.98, p = 7.91×10^{-8}, FDR = 1.49×10^{-5}), a pleiotropic cytokine previously shown to be expressed in the endometrium and decidua (*Figure 3A* and *Table 2*; *Kitaya et al., 2000*; *Okada et al., 2000*; *Dunn et al., 2002*; *Okada et al., 2004*; *Godbole and Modi, 2010*). *IL15* was robustly expressed at the first trimester maternal-fetal interface in stromal fibroblast lineage cells (*Figure 4A*), and there was a general correlation between *HAND2* and *IL15* expression in single cells (*Figure 4A* inset) (*Vento-Tormo et al., 2018*). IL15 protein localized to cytoplasm in ESF lineage cells in human pregnant decidua (*Figure 4B*) in Human Protein Atlas IHC data. The *IL15* promoter loops to several distal sites in H3K27ac HiChIP data from E6E7hTERT endometrial cells including to regions bound by PGR, NR2F2, GATA2, FOSL2, FOXO1, and SRC2, an intrinsic histone acetyltransferase that is a

Table 1. Genes dysregulated by *HAND2* knockdown are enriched in pathways relevant to endometrial stromal cells and pregnancy in general.

Enriched pathway	Roles in ESFs and pregnancy	References
Wnt Signaling	Decidualization	*Peng et al., 2008*; *Hayashi et al., 2009*; *Sonderegger et al., 2010*; *Franco et al., 2011*; *Wang et al., 2013*
BMP Signaling	Decidualization	*Ying and Zhao, 2000*; *Lee et al., 2007*; *Li et al., 2007*; *Wetendorf and DeMayo, 2012*
ErbB Signaling	Decidualization	*Lim et al., 1997*; *Klonisch et al., 2001*; *Large et al., 2014*
TGF-beta Receptor Signaling	Decidualization	*Jones et al., 2006*; *Li, 2014*; *Ni and Li, 2017*
BMP2-WNT4-FOXO1 Pathway in Human Primary Endometrial Stromal Cell Differentiation	Decidualization	*Gellersen and Brosens, 2003*; *Buzzio et al., 2006*; *Lee et al., 2007*; *Li et al., 2007*; *Brayer et al., 2011*; *Lynch et al., 2009*; *Kajihara et al., 2013*
AGE/RAGE Pathway	Placental bed development disorders Preeclampsia Induction of pro-inflammatory factors via nuclear factor-κB (NFκB)	*Chekir et al., 2006*; *Lappas et al., 2007*; *Oliver et al., 2011*; *Guedes-Martins et al., 2013*
Aryl Hydrocarbon Receptor Pathway	Mediation of maternal immunotolerance to fetal allograft	*Munn et al., 1998*; *Abbott et al., 1999*; *Funeshima et al., 2005*; *Hao et al., 2013*
Circadian Rhythm Related Genes	Implantation and parturition	*Roizen et al., 2007*; *Olcese, 2012*; *Olcese et al., 2013*; *Greenhill, 2014*; *Menon et al., 2016*
RAC1/PAK1/p38/MMP2 Pathway	Decidual inflammation, senescence and parturition	*Menon et al., 2016*

Table 2. Exemplar genes differentially expressed in ESFs upon siRNA-mediated *HAND2* knockdown.

Mean, base mean expression level. FC, $\log_2$ fold change. SE, standard error in $\log_2$ fold change. WS, Wald statistic. p-Value, Wald test p-value. Adj-p, Benjamini-Hochberg (BH) adjusted p-value. Function, function of gene inferred from Wikipathway 2019 human annotation. Association with preterm birth (PTB, HP:0001622) and premature rupture of membranes (PROM, HP:0001788) inferred from human phenotype ontology annotation*.

Gene	Mean	FC	SE	WS	p-Value	Adj-p	Function
ARNT2	44.47	1.20	0.28	4.30	1.73E-05	1.89E-03	AHR signaling / Circadian rhythm
ARNTL	42.52	−2.95	0.80	−3.67	2.46E-04	1.79E-02	AHR signaling / Circadian rhythm
IL15	63.31	7.98	1.49	5.37	7.91E-08	1.49E-05	Cell migration
BMP4	58.10	−8.34	1.25	−6.66	2.75E-11	8.28E-09	Decidualization
GSK3B	69.23	−5.53	1.48	−3.73	1.94E-04	1.49E-02	Decidualization
HAND2	136.06	−1.63	0.18	−8.85	9.10E-19	7.64E-16	Knocked down gene
CHUK	765.77	0.44	0.14	3.14	1.67E-03	7.94E-02	NFκB pathway
IκBKE	9.91	−5.41	1.65	−3.27	1.06E-03	5.72E-02	NFκB pathway
MYD88	95.02	−0.93	0.26	−3.55	3.88E-04	2.59E-02	NFκB pathway
NFκBIE	106.63	−0.78	0.25	−3.08	2.10E-03	9.53E-02	NFκB pathway
RTKN2	50.64	8.02	1.33	6.02	1.75E-09	4.05E-07	NFκB pathway
CRKL	1278.85	−0.31	0.09	−3.31	9.21E-04	5.10E-02	PTB
EOGT	233.65	−2.77	0.80	−3.45	5.63E-04	3.38E-02	PTB
LMNA	773.24	6.97	1.57	4.44	8.92E-06	1.06E-03	PTB; PROM
PEX11B	181.31	10.05	1.12	9.00	2.28E-19	2.06E-16	PTB
SERPINH1	1654.90	−6.01	1.31	−4.59	4.40E-06	5.61E-04	PROM
SLC17A5	826.28	0.76	0.13	5.81	6.34E-09	1.40E-06	PTB
ZMPSTE24	2140.67	−0.19	0.05	−4.10	4.10E-05	3.92E-03	PTB; PROM

*Extended list of genes associated with the pathologies of pregnancy and their expression levels can be found in **Table 2—source data 1** used to generate **Figures 2G** and **4G**. (GSE26787 = recurrent spontaneous abortion [RSA] and implantation failure [IF]; GSE91077 = ESFs and DSCs from women with preeclampsia [PE]).

The online version of this article includes the following source data for Table 2:

Source data 1. Differential expression of genes in RSA, IF and PE (in ESFs and DSCs) in relation to genes differentially expressed upon *HAND2* knockdown in ESFs.

transcriptional co-factor of ligand-dependent hormone receptors (*Figure 4C*; see Materials and methods for references). The *IL15* promoter also loops to a putative enhancer in its first intron that contains a PGR-binding site and SNPs marginally associated with a maternal effect on offspring birth weight (rs190663174, $p = 6 \times 10^{-4}$) by GWAS (*Warrington et al., 2019*). *IL15* was significantly upregulated by *in vitro* decidualization of human ESFs into DSCs by cAMP/progesterone treatment ($\text{Log}_2\text{FC} = 2.15$, $p = 2.58 \times 10^{-33}$, $\text{FDR} = 1.59 \times 10^{-31}$), and significantly downregulated by siRNAs targeting PGR ($\text{Log}_2\text{FC} = -1.24$, $p = 6.23 \times 10^{-15}$, $\text{FDR} = 1.80 \times 10^{-13}$) and GATA2 ($\text{Log}_2\text{FC} = -2.08$, $p = 4.16 \times 10^{-3}$, $\text{FDR} = 0.14$) (*Figure 4D*), but not NR2F2 ($\text{Log}_2\text{FC} = 0.19$, $p = 0.38$, $\text{FDR} = 0.93$) or FOXO1 ($\text{Log}_2\text{FC} = 0.29$, $p = 0.04$, $\text{FDR} = 0.22$) (*Figure 4D*; see Materials and methods for references). Although HAND2 binding data is not available for human stromal fibroblast lineage cells, several HAND2 binding motifs (≥ 0.85 motif match) are located within enhancers that loop to the *IL15* promoter.

Differential *IL15* expression throughout the menstrual cycle and pregnancy

Our observations that *HAND2* is progesterone responsive and differentially expressed throughout the menstrual cycle and pregnancy suggest that *IL15*, which is controlled by HAND2 as well as cAMP/progesterone/PGR/GATA2, may be similarly regulated. Indeed, like *HAND2*, we found that *IL15* expression increased as the menstrual cycle progressed, peaking in the middle-late secretory phases (*Figure 4E*; *Talbi et al., 2006*) and decreased in expression from the first trimester to term
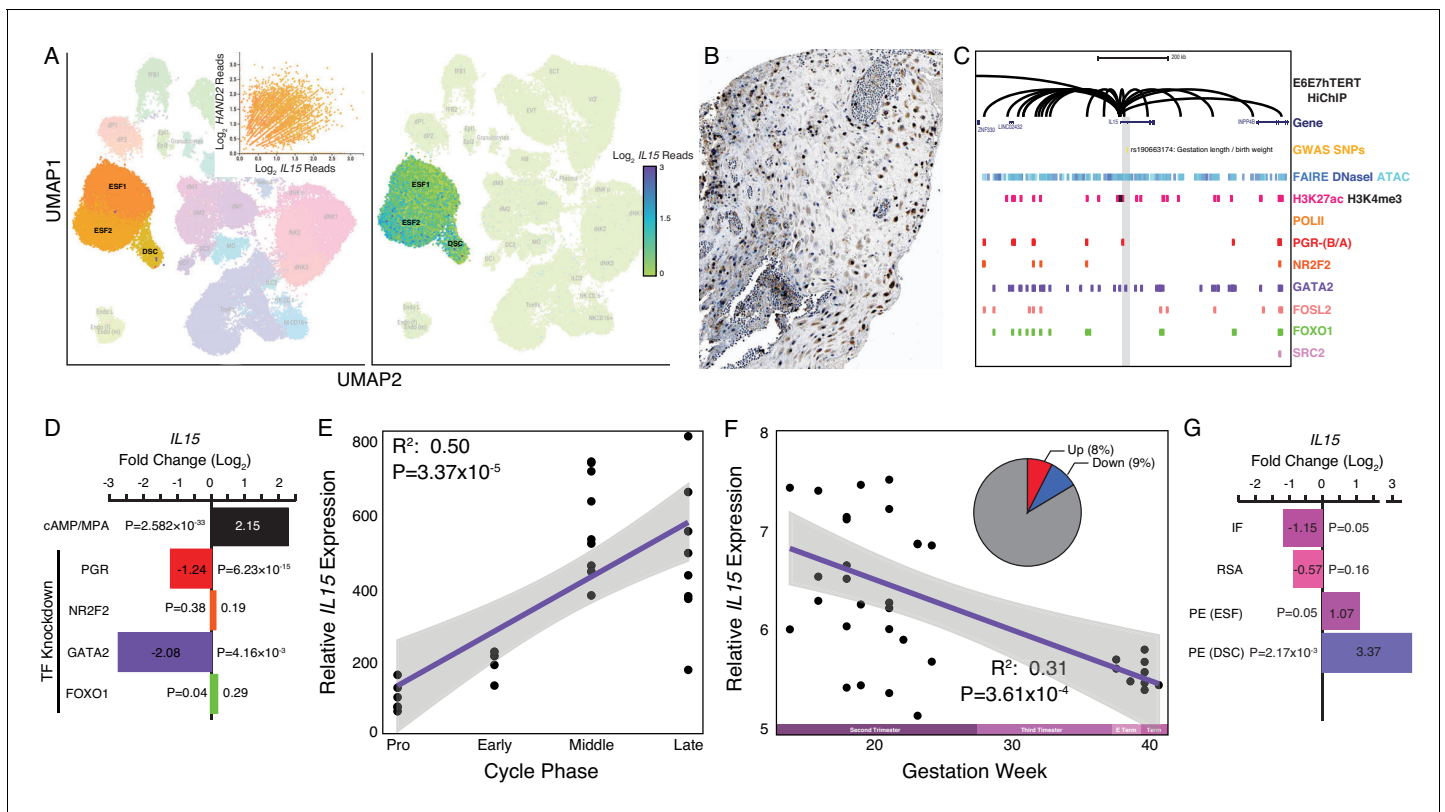
Figure 4. Expression of *IL15* at the maternal-fetal interface. (**A**) UMAP clustering of scRNA-Seq data from human first trimester maternal-fetal interface. Left, clusters colored according to inferred cell type. The ESF1, ESF2, and DSC clusters are highlighted. Inset, per cell expression of *HAND2* and *IL15* in ESF1s, ESF2s, and DSCs. Right, cells within clusters are colored according to *IL15* expression level. scRNA-Seq data from *Vento-Tormo et al., 2018*. (**B**) IL15 protein expression in human pregnant decidua, with strong cytoplasmic staining in endometrial stromal cells. Image credit: Human Protein Atlas. (**C**) Regulatory landscape of the *IL15* locus. Chromatin loops inferred from H3K27ac HiChIP, regions of open chromatin inferred from FAIRE-, DNaseI-, and ATAC-Seq, and the locations of histone modifications and transcription factor ChIP-Seq peaks are shown. The location of an SNP associated with gestation length / birth weight is also shown (highlighted in gray). Note that the *IL15* promoter forms many long-range loops to regions marked by H3K27ac and bound by PGR, NR2F2 (COUP-TFII), GATA2, FOSL2, FOXO1, and SRC2. (**D**) *IL15* expression is upregulated by *in vitro* decidualization of ESFs into DSC by cAMP/progesterone treatment, and downregulated by siRNA-mediated knockdown of PGR and GATA2 but not NR2F2 or FOXO1. n = 3 per transcription factor knockdown. (**E**) Relative expression of *IL15* in the proliferative (n = 6), early (n = 4), middle (n = 9), and late (n = 8) secretory phases of the menstrual cycle. Note that outliers are excluded from the figure but not the regression; 95% CI is shown in gray. Gene expression data from *Talbi et al., 2006*. (**F**) Relative expression of *IL15* in the basal plate from mid-gestation to term (14–40 weeks, n = 36); 95% CI is shown in gray. Inset, percent of up- (Up) and downregulated (Down) genes between weeks 14–19 and 37–40 of pregnancy (FDR ≤ 0.10). Gene expression data from *Winn et al., 2007*. (**G**) *IL15* expression is significantly upregulated in DSCs from women with preeclampsia (PE, n = 5) compared to healthy controls (n = 5), while it is only marginally upregulated in ESFs from the same patient group. It is also marginally downregulated in the endometria of women with implantation failure (IF, n = 5) and it is not differentially expressed in the endometria of women with recurrent spontaneous abortion (RSA, n = 5) compared to fertile controls (n = 5). Gene expression data for RSA and IF from *Lédée et al., 2011* and for PE from *Garrido-Gomez et al., 2017*.

© 2021, Human Protein Atlas. Figure 4B is adapted from the Human Protein Atlas (top image cropped, image color auto adjusted). Published under a CC BY SA 3.0 unported license.

(*Figure 4F*; *Winn et al., 2007*). *IL15* expression was also dysregulated in the endometria of women with implantation failure but not recurrent spontaneous abortion, compared to fertile controls (*Figure 4G*; *Lédée et al., 2011*). In women with preeclampsia, *IL15* was not dysregulated in ESFs, but it was expressed significantly higher in DSCs, compared to controls (*Figure 4G*; *Garrido-Gomez et al., 2017*). Thus, like *HAND2*, *IL15* is differentially expressed throughout the menstrual cycle and pregnancy, and in the endometria of women with implantation failure.

ESF-derived IL15 promotes NK and trophoblast migration

Endometrial stromal cells promote the migration of uterine natural killer (uNK) (*Chen et al., 2011*) and trophoblast cells (*Graham and Lala, 1991*; *Paiva et al., 2009*; *Zhu et al., 2009*; *Godbole et al., 2011*). IL15, in particular, stimulates the migration of uNK cells (*Allavena et al., 1997*; *Verma et al., 2000*; *Ashkar et al., 2003*; *Barber and Pollard, 2003*; *Kitaya et al., 2005*) and the human chorio-carcinoma cell line, JEG-3 (*Zygmunt et al., 1998*). Therefore, we tested whether ESF-derived IL15 influenced the migration of primary human NK cells and immortalized first trimester extravillous trophoblasts (HTR-8/SVneo) in trans-well migration assays (*Figure 5A*). We found that ESF media supplemented with recombinant human IL15 (rhIL15) was sufficient to stimulate the migration of NK and HTR-8/SVneo cells to the lower chamber of trans-wells, compared to non-supplemented media (*Figure 5B,C* and *Figure 5—source data 1*, *2*). Conditioned media from ESFs with siRNA-mediated *HAND2* knockdown increased migration of both NK and HTR-8/SVneo compared to negative control (i.e. non-targeting siRNA; *Figure 5B,C*). Conditioned media from ESFs with siRNA-mediated *IL15* knockdown reduced migration of both NK and HTR-8/SVneo cells compared to negative control (*Figure 5B,C*). Similarly, ESF conditioned media supplemented with anti-IL15 antibody reduced cell migration compared to media supplemented with control IgG antibody (*Figure 5B,C*).

Discussion

Eutherian mammals evolved a suite of traits that support pregnancy, including an interrupted estrous cycle allowing for prolonged gestation lengths, maternal-fetal communication, implantation, maternal immunotolerance and recognition of pregnancy, and thus are uniquely afflicted by disorders of these processes. When searching for clues as to how variation in normal physiological functions can lead to dysfunction and disease, deeper understanding of the evolutionary and developmental histories of organ and tissues has the potential to provide novel insights. Here, we used evolutionary transcriptomics to identify genes that evolved to be expressed on the maternal side (endometrium) of the maternal-fetal interface during the origins of pregnancy in Eutherians, and hence may also contribute to pregnancy complications such as infertility, recurrent spontaneous abortion, and preterm birth.

Among the genes recruited into endometrial expression in Eutherians, we identified *HAND2*, a pleiotropic transcription factor that plays an essential role in suppressing estrogen signaling at the time of uterine receptivity to blastocyst embedding, through its down-regulation of pro-estrogenic genes and by directly inhibiting the transcriptional activities of the estrogen receptor (*Huyen and Bany, 2011*; *Li et al., 2011*; *Shindoh et al., 2014*; *Fukuda et al., 2015*; *Mestre-Citrinovitz et al., 2015*; *Murata et al., 2019*). Consistent with these functions, we found evidence of estrogen activity in the endometrium of pregnant opossum. Earlier research detected similar activity in the gravid oviduct of birds and reptiles (*Means et al., 1975*; *Kato et al., 1992*; *Girling, 2002*; *González-Morán, 2015*). These data indicate that suppression of estrogen signaling during the window of uterine receptivity to implantation is an evolutionary innovation of Eutherian mammals, which involved the recruitment of *HAND2* and its anti-estrogenic functions into endometrial expression.

The roles of *HAND2* in DSCs and implantation are well-understood (*Huyen and Bany, 2011*; *Li et al., 2011*; *Shindoh et al., 2014*; *Fukuda et al., 2015*; *Mestre-Citrinovitz et al., 2015*; *Murata et al., 2019*; *Šućurović et al., 2020*). In contrast, the function(s) of *HAND2* at other stages of pregnancy and in ESFs remain relatively unexplored, despite the persistence of ESFs in the pregnant endometrium until term (*Richards et al., 1995*; *Suryawanshi et al., 2018*; *Muñoz-Fernández et al., 2019*; *Sakabe et al., 2020*). *HAND2*, for example, plays a role in orchestrating the transcriptional response to progesterone during decidualization (*Huyen and Bany, 2011*; *Li et al., 2011*; *McConaha et al., 2011*; *Shindoh et al., 2014*; *Murata et al., 2020*). Similarly, *Hand2* knockout mice are infertile because of persistent estrogen signaling during the window of implantation, leading to implantation failure (*Li et al., 2011*; *Jones et al., 2013*). The functions of *Hand2* at other stages of pregnancy could unfortunately not be explored in these *Hand2* knockout mice as the conditional targeting strategy knocks out *Hand2* in *Pgr*-expressing cells. *Hand2* expression is thereby eliminated upon initiation of *Pgr* expression in the uterus, coincident with the onset of sexual maturity.

We knocked down *HAND2* in ESFs and found that downstream dysregulated genes were enriched for human phenotype ontologies related to disorders of pregnancy, including 'Premature
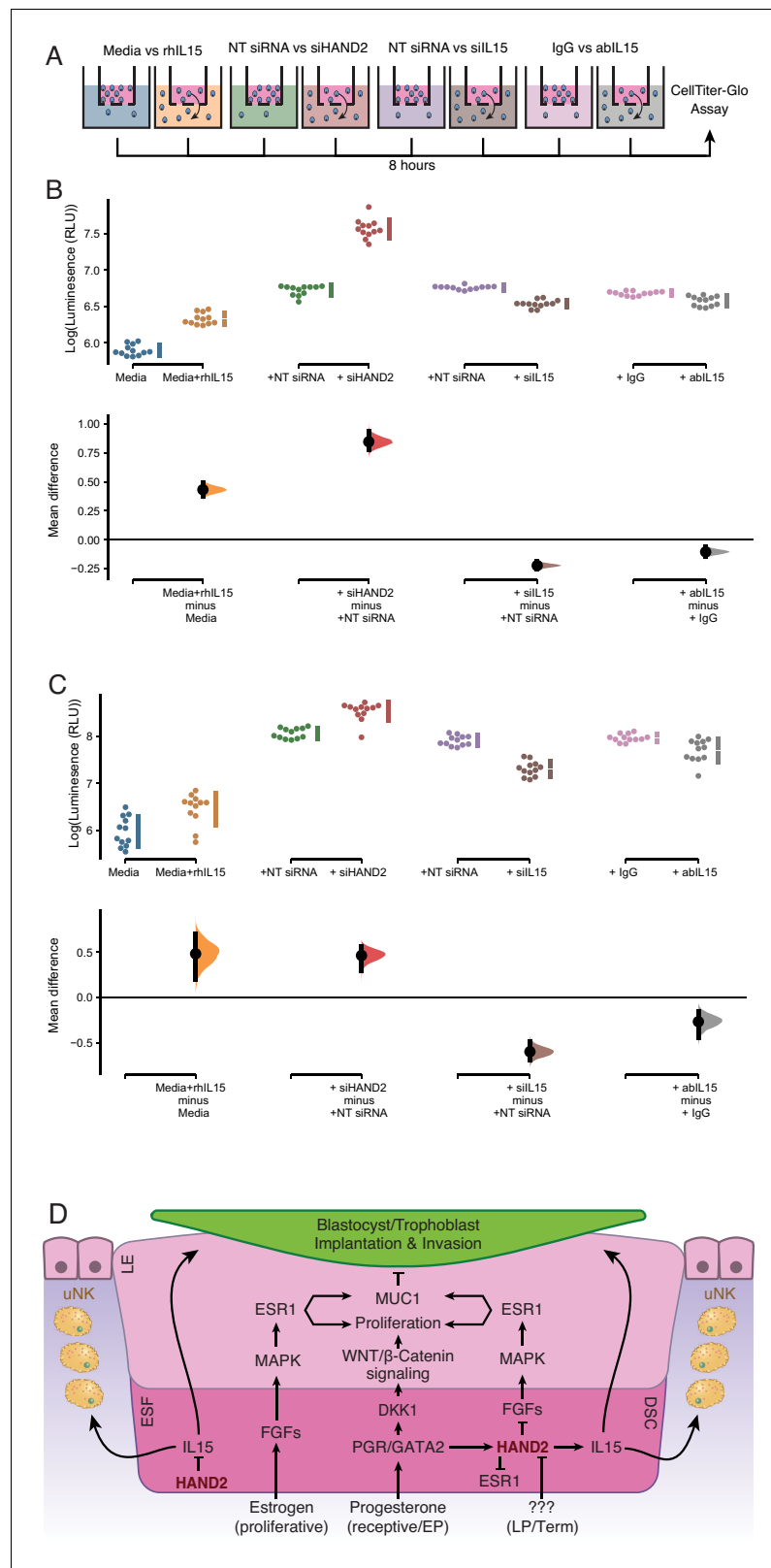
Figure 5. ESF-derived IL15 promotes NK and trophoblast migration in trans-well assays. (**A**) Cartoon of trans-well migration assay comparisons. Cells that migrated to the lower chamber were quantified using the CellTiter-Glo luminescent cell viability assay after 8 hr. (**B**) Primary natural killer (NK) cells. Raw luminescence data (RLU) from cells in the lower chamber is shown in the upper panel, mean difference (effect size) in experiment minus control

Figure 5 continued on next page

Figure 5 continued

luminescence values are shown as dots with the 95% confidence interval indicated by vertical bars in the lower panel; distribution estimated from 5000 bootstrap replicates. The mean difference between Media and media supplemented with recombinant human IL15 (Media+rhIL15) is 0.432 [95.0% CI: 0.376–0.492]; p = 0.00. The mean difference between ESFs transiently transfected with non-targeting siRNA (NT siRNA) and *HAND2*-specific siRNAs (siHAND2) is 0.847 [95.0% CI: 0.774–0.936]; p = 0.00. The mean difference between ESFs transiently transfected with NT siRNA and IL15-specific siRNAs (siIL15) is −0.223 [95.0% CI: −0.256 − −0.192]; p = 0.00. The mean difference between ESF media neutralized with a non-specific antibody (IgG) or IL15-specific antibody (abIL15) is −0.106 [95.0% CI: −0.147 − −0.067]; p = 0.00. n = 12. (C) Extravillous trophoblast cell line HTR-8/SVneo. Raw luminescence data (RLU) from cells in the lower chamber is shown in the upper panel, mean difference (effect size) in experiment minus control luminescence values are shown as dots with the 95% confidence interval indicated by vertical bars in the lower panel; distribution estimated from 5000 bootstrap replicates. The mean difference between Media and Media+rhIL15 is 0.482 [95.0% CI: 0.193–0.701]; p = 0.002. The mean difference between ESFs transiently transfected with NT siRNA and siHAND2 is 0.463 [95.0% CI: 0.291–0.559]; p = 0.00. The mean difference between ESFs transiently transfected with NT siRNA and siIL15 is −0.598 [95.0% CI: −0.698–0.490]; p = 0.00. The mean difference between ESF media neutralized with IgG or abIL15 is −0.267 [95.0% CI: −0.442 − −0.151]; p = 0.0004. n = 12. (D) Model of HAND2 functions in the endometrium. During the proliferative phase HAND2 inhibits *IL15*, and thus the migration of uNK and trophoblast cells. In the receptive phase, HAND2 activates *IL15*, which promotes migration of uNK and trophoblast cells. In the receptive phase and early pregnancy (EP), HAND2 suppresses estrogen signaling by down-regulating *FGF*s and directly binding and inhibiting the ligand-dependent transcriptional activation function of ESR1. During late pregnancy/term (LP/Term), reduced HAND2 expression mitigates its anti-estrogenic functions. Parturition signal unknown (???). ESF = endometrial stromal fibroblasts (proliferative phase), DSC = decidual stromal cells (receptive phase), LE = luminal epithelium.

The online version of this article includes the following source data for figure 5:

Source data 1. Raw and log transformed luminescence data for NK trans-well migration assays.
Source data 2. Raw and log transformed luminescence data for HTR-8 trans-well migration assays.

Rupture of Membranes', 'Premature Birth', and 'Abnormal Delivery', suggesting that *HAND2* has functions throughout pregnancy and in parturition. Indeed, we discovered that SNPs recently implicated in the regulation of gestation length and birth weight by GWAS (*Warrington et al., 2019*; *Sakabe et al., 2020*) make long-range interactions to the *HAND2* promoter. Also of note, *HAND2* expression is significantly higher in placental villous samples from idiopathic spontaneous preterm birth (isPTB) compared to term controls (*Brockway et al., 2019*). However, this difference may be related to gestational age rather than the etiology of PTB (*Eidem et al., 2016*).

Additionally, analyzing previously published datasets we noticed that *HAND2* expression decreases throughout gestation. Unlike the majority of Eutherians, where parturition closely follows the significant drop in progesterone concentrations in maternal peripheral blood, this is not the case for humans and other Old World primates (*Ratajczak et al., 2010*), where progesterone levels keep rising throughout gestation, reaching maximum at birth. These observations, combined with the central role of *HAND2* in mediating the anti-estrogenic actions of progesterone, suggest decreased *HAND2* at the end of pregnancy may contribute to the estrogen-dominant uterine environment at the onset of labor (*Pinto et al., 1966*; *Pepe and Albrecht, 1995*; *Mesiano et al., 2002*; *Smith et al., 2009a*; *Ratajczak et al., 2010*; *Welsh et al., 2012*), despite high systemic progesterone. Low *HAND2* at the end of pregnancy in humans is therefore most likely not directly related to progesterone concentrations, suggesting that an unidentified inhibitory signal reduces endometrial *HAND2* expression. While taken collectively these data indicate a role for *HAND2* in pre/term birth, a direct mechanistic link between *HAND2* expression and the timing of parturition remains to be demonstrated.

One of the genes dysregulated by *HAND2* knockdown was the multifunctional cytokine *IL15*, which plays important roles in innate and adaptive immunity. In the context of pregnancy, it is important for the recruitment of uterine natural killer (uNK) cells to the endometrium (*Kitaya et al., 2000*; *Verma et al., 2000*; *Ashkar et al., 2003*; *Barber and Pollard, 2003*; *Kitaya et al., 2005*; *Laskarin et al., 2006*). The roles of uNK cells in the remodeling of uterine spiral arteries and regulating trophoblast invasion are well known (*Zygmunt et al., 1998*; *Hanna et al., 2006*; *Smith et al., 2009b*; *Burke et al., 2010*; *Hazan et al., 2010*; *Lash et al., 2010*; *Bany et al., 2012*; *Robson et al.,*

2012; *Zhang et al., 2013*; *Lima et al., 2014*; *Fraser et al., 2015*; *Felker and Croy, 2016*; *Renaud et al., 2017*). Endometrial stromal cell-derived IL15 is also necessary for the selective targeting and clearance of senescent endometrial stromal cells from the implantation site by uNK cells, which is essential for endometrial rejuvenation and remodeling at embryo implantation (*Brighton et al., 2017*). Dysregulation of uNK cell-mediated clearance of these senescent cells has also been implicated in recurrent pregnancy loss (*Lucas et al., 2020*). We found that, like *HAND2*, *IL15* decreases throughout gestation and both genes increase in expression as the menstrual cycle progresses.

Unexpectedly, however, while previous studies showed that *HAND2* induces *IL15* in DSCs (*Shindoh et al., 2014*; *Murata et al., 2020*), we discovered that *HAND2* inhibited *IL15* expression in ESFs, indicating a switch in regulatory activity sometime during early menstrual cycle. These data suggest that *HAND2* regulates the appropriate timing of endometrial *IL15* expression during the menstrual cycle and throughout pregnancy, and thus the appropriate timing of uNK cell recruitment, trophoblast migration and the clearance of senescent endometrial stromal cells from the implantation site (*Figure 5D*). While the signals that initiate parturition in humans and other Catarrhine primates are unknown, it has been proposed that a 'decidual clock' may regulate the successful establishment and maintenance of pregnancy, such that severe decidualization defects lead to infertility, moderate defects lead to recurrent pregnancy loss/recurrent spontaneous abortion, and mild defects lead to preterm birth (*Norwitz et al., 2015*). Our results suggest that part of this clock may be the transition of ESFs that persist in the endometrium during pregnancy to DSCs, and/or DSCs into senescent DSCs (snDSCs) which no longer express *IL15* (*Lucas et al., 2020*), leading to a shift in the balance of tolerizing immune cells at the maternal-fetal interface and thus withdrawal of maternal immunotolerance of the fetal allograft. Thus, our observation of low *HAND2* and *IL15* near term may reflect a reduction of anti-inflammatory DSCs (high *HAND2* and *IL15*) and an accumulation of pro-inflammatory snDSCs (low *HAND2* and *IL15*) at the maternal-fetal interface. Additional work is needed to elucidate the mechanisms that underlie change in *HAND2-IL15* dynamics and determine whether these progressive cell state changes occur during gestation.

Decreased *HAND2* and *IL15* expression near term and their influence on immune cells at the maternal-fetal interface may also play a role in parturition. Pre/term labor is known to be associated with elevated inflammation and an influx of immune cells into utero-placental tissues (*Thomson et al., 1999*; *Young et al., 2002*; *Osman et al., 2003*; *Gomez-Lopez et al., 2010*; *Rinaldi et al., 2011*; *Rinaldi et al., 2015*; *Hamilton et al., 2012*; *Shynlova et al., 2013*; *Bartmann et al., 2014*; *Menon et al., 2016*; *Peters et al., 2016*; *Wilson and Mesiano, 2020*). uNK cells are abundant throughout gestation (*Bulmer et al., 1991*; *King et al., 1991*; *Moffett-King, 2002*; *Williams et al., 2009*; *Bartmann et al., 2014*), but whether they play a role in late pregnancy and parturition is unclear. However, depletion of uNK cells rescues LPS-induced preterm birth in *IL10*-null mice (*Murphy et al., 2005*), indicating they contribute to infection/inflammation-induced preterm parturition (*Murphy et al., 2009*). CD16$^+$CD56^{dim} (cytotoxic) uNK cells have also been observed in the decidua and the placental villi of women with preterm but not term labor, suggesting an association between dysregulation of uNK cells and preterm birth in humans (*Gomaa et al., 2017*). uNK cells are associated with other pregnancy complications in humans such as fetal growth restriction, preeclampsia, and recurrent spontaneous abortion (*Moffett et al., 2004*; *Hiby et al., 2010*; *Wallace et al., 2013*; *Wallace et al., 2014*; *Kieckbusch et al., 2014*). Taken together, these data indicate that uNK cells may act downstream of *HAND2-IL15* signaling in the timing of parturition.

Conclusions

Here, we show that *HAND2* evolved to be expressed in endometrial stromal cells in the Eutherian stem-lineage, coincident with the evolution of suppressed estrogen signaling during the window of implantation and an interrupted reproductive cycle during pregnancy, which necessitated a means to regulate the length of gestation. Our data suggest that *HAND2* may contribute to the regulation of gestation length by promoting an estrogen dominant uterine environment near term and through its effect on IL15 signaling and uNK cell function. To further expand our understanding of *HAND2* functions at the molecular mechanistic level, multiple technical and ethical difficulties associated with studying human pregnancy *in vivo* will need to be overcome. Therefore, recently developed organoid models of the human maternal-fetal interface (*Rinehart et al., 1988*; *Boretto et al., 2017*;

Turco et al., 2017; *Turco et al., 2018*; *Marinić et al., 2020*), which allow for *in vitro* 3D manipulation, will be instrumental.

Materials and methods

Endometrial gene expression profiling and ancestral transcriptome reconstruction

Data collection

We obtained previously generated RNA-Seq data from endometria of amniotes by searching NCBI BioSample, Sequence Read Archive (SRA), and Gene Expression Omnibus (GEO) databases for anatomical terms referring to the portion of the female reproductive tract (FRT), including 'uterus', 'endometrium', 'decidua', 'oviduct', and 'shell gland', followed by manual curation to identify those datasets that included the FRT region specialized for maternal-fetal interaction or shell formation. Datasets that did not indicate whether samples were from pregnant or gravid females were excluded, as were those composed of multiple tissue types. Species included in this study and their associated RNA-Seq accession numbers are included in *Figure 1—source data 1*.

New RNA-Seq data

Endometrial tissue samples from the pregnant uteri of baboon (n = 3), mouse (n = 3), hamster (n = 3), bat (n = 2), and squirrel (n = 2) were dissected and mailed to the University of Chicago in RNA-Later. These samples were further dissected to remove myometrium, luminal epithelium, and extra-embryonic tissues, and then washed three times in ice cold PBS to remove unattached cell debris and red blood cells. Total RNA was extracted from the remaining tissue using the RNeasy Plus Mini Kit (74134, QIAGEN) per manufacturer's instructions. RNA concentrations were determined by Nanodrop 2000 (Thermo Scientific). A total amount of 2.5 µg of total RNA per sample was submitted to the University of Chicago Genomics Facility for Illumina Next Gen RNA sequencing. Quality was assessed with the Bioanalyzer 2100 (Agilent). A total RNA library was generated using the TruSEQ stranded mRNA with RiboZero depletion (Illumina) for each sample. The samples were fitted with one of six different adapters with a different 6-base barcode for multiplexing. Completed libraries were run on an Illumina HiSEQ2500 with v4 chemistry on two replicate lanes for hamster and one lane for other species of an eight lane flow cell, generating 30–50 million 50 bp single-end reads per sample.

Multispecies RNA-Seq analysis

For all RNA-Seq analyses, we used Kallisto (*Bray et al., 2016*) version 0.42.4 to pseudo-align the raw RNA-Seq reads to reference transcriptomes (see *Figure 1—source data 1* for reference genome assemblies) and to generate transcript abundance estimates. We used default parameters bias correction, and 100 bootstrap replicates. Kallisto outputs consist of transcript abundance estimates in Transcripts Per Million (TPM), which were used to determine gene expression.

Ancestral transcriptome reconstruction

We previously showed that genes with TPM $\geq$ 2.0 are actively transcribed in endometrium while genes with TPM < 2.0 lack hallmarks of active transcription such as promoters marked with H3K4me3 (*Wagner et al., 2012*; *Wagner et al., 2013*). Based on these findings, we transformed values of transcript abundance estimates into discrete character states, such that genes with TPM $\geq$ 2.0 were coded as expressed (state = 1), genes with TPM < 2.0 were coded as not expressed (state = 0), and genes without data in specific species coded as missing (state = ?). The binary encoded endometrial gene expression dataset generally grouped species by phylogenetic relatedness, suggesting greater signal-to-noise ratio than raw transcript abundance estimates. Therefore, we used the binary encoded endometrial transcriptome dataset to reconstruct ancestral gene expression states and trace the evolution of gene expression gains (0 → 1) and losses (1 → 0) in the endometria across vertebrate phylogeny (*Figure 1A*). We used Mesquite (*Maddison and Maddison, 2019*) (v3.02) with parsimony optimization to reconstruct ancestral gene expression states, and identify genes that gained or lost endometrial expression. Expression was classified as an unambiguous gain if a gene

was not inferred as expressed at a particular ancestral node (state = 0) but inferred as expressed (state = 1) in a descendent of that node, and vice versa for the classification of a loss of endometrial expression (*Figure 1—source data 2*). Parsimony optimization of ancestral states results in three ancestral state reconstructions (ASRs): 'ambiguous', 'most-parsimonious', and 'unambiguous'. An ambiguous ASR is not resolved and interpreted as unknown, a most-parsimonious ASR is 'potentially' the ASR but not necessarily so because other ancestral states are also possible, while an unambiguous ASR is the most-optimal state such that alternative ASRs can be rejected. The criterion for determining which genes belong in these categories was the parsimony optimization method implemented in Mesquite (v3.02). We thus identified 149 genes that unambiguously evolved endometrial expression in the stem-lineage of Eutherian mammals (*Figure 1—source data 3*).

Pathway enrichments

We used WebGestalt v. 2019 (*Liao et al., 2019*) to determine if the 149 identifies genes were enriched in ontology terms using over-representation analysis (ORA). A key advantage of WebGestalt is that it allowed for the inclusion of a custom background gene list, which was the set of 21,750 genes for which we could reconstruct ancestral states, rather than all annotated protein-coding genes in the human genome. We used ORA to identify enriched terms for three pathway databases (KEGG, Reactome, and Wikipathway), the Human Phenotype Ontology database, and a custom database of genes implicated in preterm birth by GWAS. The preterm birth gene set was assembled from the NHGRI-EBI Catalog of published genome-wide association studies (GWAS Catalog), including genes implicated in GWAS with either the ontology terms 'Preterm Birth' (EFO_0003917) or 'Spontaneous Preterm Birth' (EFO_0006917), as well as two recent preterm birth GWAS (*Warrington et al., 2019*; *Sakabe et al., 2020*) using a genome-wide significant p-value of 9×10^{-6}. The custom gmt file used to test for enrichment of preterm birth associated genes is included as a supplementary data file to *Figure 1* (*Figure 1—source data 8*).

Marsupial gene expression analysis

Opossum uterine gene expression time course

To explore the expression of *HAND2* and other genes throughout gestation in Marsupials, we analyzed previously generated short-tailed opossum (*Monodelphis domestica*) RNA-Seq data from virgin non-pregnant (SRR2972837, SRR2972848), day 7 (during the histotrophic phase; SRP111668), day 12.5 (just after hatching and during the transition from the histotrophic to the placental phase; GSM1611397), day 13 (early placental phase; SRP111668), day 13.5–14.5 (during the late placental to early parturition phase; SRR2969483, SRR2969536, SRR2970443), and 9–10 month postpartum utera (SRR2972728 and SRR2972729) (*Figure 1—source data 7*; *Lynch et al., 2015*; *Hansen et al., 2016*; *Griffith et al., 2017*; *Griffith et al., 2019*).

Wallaby RNA-Seq data from non-pregnant and pregnant animals

RNA-Seq data for tammar wallaby (*Macropus eugenii*) uterine tissue from pregnant and non-pregnant animals were from PRJDB1934.

RNA-Seq analysis

We used Kallisto version 0.42.4 to pseudo-align RNA-Seq reads to the *M. domestica* and *M. eugenii* reference transcriptomes with default parameters bias correction and 100 bootstrap replicates. Kallisto output quantifies transcript abundance estimates in TPM.

Immunohistochemistry (IHC)

Endometrial tissue from pregnant opossum (12.5d) was fixed in 10% neutral-buffered formalin, paraffin-embedded, sectioned at 4 µm, and mounted on slides. Paraffin sections were dried at room temperature overnight and then baked for 12 hr at 50°C. Prior to immunostaining, de-paraffinization and hydration were done in xylene and graded ethanol to distilled water. During hydration, a 5 min blocking for endogenous peroxidase was done in 0.3% H_2O_2 in 95% ethanol. Antigen retrieval was performed in retrieval buffer pH 6, using a pressure boiler microwave as a heat source with power set to full, allowing retrieval buffer to boil for 20 min, and then cooled in a cold water bath for 10 min. To stain sections, we used the Pierce Peroxidase IHC Detection Kit (cat # 36000) following

the manufacturer's protocol. Briefly, uterine sections were incubated at 4°C overnight with polyclonal antibodies against HAND2 (Santa Cruz SC-9409), MUC1 (Novus Biologicals NB120-15481), p-ERα (Santa Cruz SC-12915), p-Erk1/2 (also known as MAPK1/2; Santa Cruz SC-23759-R) at 1:1000 dilution in blocking buffer. The next day sections were washed 3x in wash buffer, and incubated with HRP-conjugated rabbit anti-mouse IgG (H+L) secondary antibody (Invitrogen cat # 31450) at 1:10,000 dilution in blocking buffer. After 30 min at 4°C, slides were washed 3x in wash buffer. Slides were developed with 1x DAB/metal concentrate and stable peroxide buffer for 5 min, then rinsed 3x for 3 min in wash buffer, and mounted with Permount (SP15-100; Thermo Fisher Scientific).

Expression of *HAND2* and *IL15* at the maternal-fetal interface

We used previously published single-cell RNA-Seq (scRNA-Seq) data from the human first trimester maternal-fetal interface (*Vento-Tormo et al., 2018*) to determine which cell types express *HAND2* and *IL15*. The dataset consists of transcriptomes for ~70,000,000 individual cells of many different cell types, including: three populations of tissue resident decidual natural killer cells (dNK1, dNK2, and dNK3), a population of proliferating natural killer cells (dNKp), type two and/or type three innate lymphoid cells (ILC2/ILC3), three populations of decidual macrophages (dM1, dM2, and dM3), two populations of dendritic cells (DC1 and DC2), granulocytes (Gran), T cells (TCells), maternal and lymphatic endothelial cells (Endo), two populations of epithelial glandular cells (Epi1 and Epi2), two populations of perivascular cells (PV1 and PV2), two endometrial stromal fibroblast populations (ESF1 and ESF2), and decidual stromal cells (DSCs), placental fibroblasts (fFB1), extravillous- (EVT), syncytio- (SCT), and villus- (VCT) cytotrophoblasts (*Figure 2A*). Data were not reanalyzed, rather previously analyzed data were accessed using the cell×gene website available at https://maternal-fetal-interface.cellgeni.sanger.ac.uk.

We note that Vento-Tormo et al. identified five populations of cells in the endometrial stromal lineage, including two perivascular populations (likely reflecting the mesenchymal stem cell-like progenitor of endometrial stromal fibroblasts and decidual stromal cells) and three cell types they call 'decidual stromal cells' and label 'dS1-3'. However, based on the gene expression patterns of 'dS1-3' (shown in Vento-Tormo et al. Figure 3a), only 'dS3' are decidualized, as indicated by expression of classical markers of decidualization such and *PRL* (*Tabanelli et al., 1992*) and *IGFBP1/2/6* (*Tabanelli et al., 1992*; *Kim et al., 1999*). In stark contrast, 'dS1' do not express decidualization markers but highly express markers of ESFs such as *TAGLN* and *ID2*, as well as markers of proliferating ESFs including *ACTA2* (*Kim et al., 1999*). 'dS2' also express ESFs markers (*TAGLN*, *ID2*, *ACTA2*), but additionally *LEFTY2* and *IGFBP1/2/6*, consistent with ESFs that have initiated the process of decidualization. These data indicate that the 'dS1' and 'dS2' populations are both ESFs, but 'dS2' are ESFs that have initiated decidualization (because they express *IGFBPs* but not *PRL*), and that 'dS3' are DSCs. Vento-Tormo et al. show that the differences in gene expression between 'dS1-3' are related to their topography in the endometrium, but degree of decidualization ('dS1'/ESF1 < 'dS2'/ESF2 < 'dS3'/DSC) is also linked to differential gene expression.

Consistent with this, other scRNA-Seq studies have identified two ESF populations and one DSC population in the first trimester decidua, and used pseudotime analyses to show that they represent different states of differentiation from ESFs to mature DSCs (*Suryawanshi et al., 2018*). Therefore, we prefer to use the ESF1/ESF2/DSC nomenclature because it more accurately reflects the biology and gene expression profile of these cell types than the 'dS1-3' naming convention. We also note that while it is generally thought that ESFs are absent from the pregnant uterus, ESFs retain a presence in the endometrium from the first trimester until term (*Richards et al., 1995*; *Suryawanshi et al., 2018*; *Muñoz-Fernández et al., 2019*; *Sakabe et al., 2020*).

Expression of HAND2 and IL15 in human decidual cells

We used previously published IHC data for HAND2 and IL15 generated from pregnant human decidua as part of the Human Protein Atlas project (http://www.proteinatlas.org/; *Uhlén et al., 2015*). Image/gene/data available from IL15 (https://www.proteinatlas.org/ENSG00000164136-IL15/tissue) and HAND2 (https://www.proteinatlas.org/ENSG00000164107-HAND2/tissue).

Functional genomic analyses of the *HAND2* and *IL15* loci

Gene expression data

We used previously published RNA-Seq and microarray gene expression data generated from human ESFs and DSCs that were downloaded from National Center for Biotechnology Information (NCBI) Sequence Read Archive (SRA) and processed remotely using Galaxy platform (https://usegalaxy.org/; Version 20.01) (*Afgan et al., 2018*) for RNA-Seq data and GEO2R. RNA-Seq datasets were transferred from SRA to Galaxy using the Download and Extract Reads in FASTA/Q format from NCBI SRA tool (version 2.10.4+galaxy1). We used HISAT2 (version 2.1.0+galaxy5; *Kim et al., 2015*) to align reads to the Human hg38 reference genome using single- or paired-end options depending on the dataset and unstranded reads, and report alignments tailored for transcript assemblers including StringTie. Transcripts were assembled and quantified using StringTie (v1.3.6) (*Pertea et al., 2015*; *Pertea et al., 2016*), with reference file to guide assembly and the 'reference transcripts only' option, and output count files for differential expression with DESeq2/edgeR/limma-voom. Differentially expressed genes were identified using DESeq2 (version 2.11.40.6+galaxy1) (*Anders and Huber, 2010*; *Love et al., 2014*). The reference file for StringTie guided assembly was wgEncodeGencodeBasicV33. GEO2R performs comparisons on original submitter-supplied processed data tables using the GEOquery (*Davis and Meltzer, 2007*) and limma (*Smyth et al., 2002*) R packages from the Bioconductor project (https://bioconductor.org/; *Gentleman et al., 2004*).

Datasets included gene expression profiles of primary human ESFs treated for 48 hr with control non-targeting, PGR-targeting (GSE94036), FOXO1-targeting (GSE94036) or NR2F2 (COUP-TFII)-targeting (GSE47052) siRNA prior to decidualization stimulus for 72 hr; transfection with GATA2-targeting siRNA was followed immediately by decidualization stimulus (GSE108407). We also explored the expression of *HAND2* and *IL5* in the endometria of women with recurrent spontaneous abortion and implantation failure using a previously published dataset (GSE26787), as well as in the endometrium throughout the menstrual cycle (GSE4888) and basal plate throughout gestation (GSE5999); HAND2 probe 220480_at, IL15 probe 205992_s_at. The expression of *HAND2* and *IL5* in ESFs and DSCs from women with normal pregnancy and severe preeclampsia was assessed from a previously generated Agilent Whole Human Genome Microarray 4 × 44K v2 dataset (GSE91077).

ChIP-Seq and open chromatin data

We used previously published ChIP-Seq data generated from human DSCs that were downloaded from NCBI SRA and processed remotely using Galaxy (*Afgan et al., 2018*). ChIP-Seq reads were mapped to the human genome (GRCh37/hg19) using HISAT2 (*Kim et al., 2015*) with default parameters and peaks called with MACS2 (*Zhang et al., 2008*; *Feng et al., 2012*) with default parameters. Samples included PLZF (GSE75115), H3K4me3 (GSE61793), H3K27ac (GSE61793), H3K4me1 (GSE57007), PGR (GSE69539), the PGR A and B isoforms (GSE62475), NR2F2 (GSE52008), FOSL2 (GSE69539), FOXO1 (GSE69542), PolII (GSE69542), GATA2 (GSE108408), SRC-2/NCOA2 (GSE123246), AHR (GSE118413), ATAC-Seq (GSE104720), and DNase1-Seq (GSE61793). FAIRE-Seq peaks were downloaded from the UCSC genome browser and not re-called.

Chromatin interaction data

To assess chromatin looping, we utilized a previously published H3K27ac HiChIP dataset from a normal hTERT-immortalized endometrial cell line (E6E7hTERT) and three endometrial cancer cell lines (ARK1, Ishikawa and JHUEM-14) (*O'Mara et al., 2019*). This study identified 66,092 to 449,157 *cis* HiChIP loops (5 kb–2 Mb in length) per cell line. The majority of loops involved interactions of over 20 kb in distance, 35–40% of loops had contact with a promoter and those promoter-associated loops had a median span >200 kb. Contact data were from the original publication and not re-called for this study. Note that *Figures 2C* and *4C* were made using a combination of the UCSC genome browser to map the location of regions of open chromatin and ChIP-Seq peaks and Illustrator to simplify the images from the genome browser.

Cell culture and *HAND2* knockdown

Human hTERT-immortalized endometrial stromal fibroblasts (T-HESC; CRL-4003, ATCC) were grown in maintenance medium, consisting of Phenol Red-free DMEM (31053–028, Thermo Fisher Scientific),

supplemented with 10% charcoal-stripped fetal bovine serum (CS-FBS; 12676029, Thermo Fisher Scientific), 1% L-glutamine (25030–081, Thermo Fisher Scientific) , 1% sodium pyruvate (11360070, Thermo Fisher Scientific), and 1x insulin-transferrin-selenium (ITS; 41400045, Thermo Fisher Scientific). A total of 2×10^5 cells were plated per well of a six-well plate and 18 hr later cells in 1750 µl of Opti-MEM (31985070, Thermo Fisher Scientific) were transfected with 50 nM of siRNA targeting *HAND2* (s18133; Silencer Select Pre-Designed siRNA; cat # 4392420, Thermo Fisher Scientific) and 9 µl of Lipofectamine RNAiMAX (133778–150, Invitrogen) in 250 µl Opti-MEM. BlockIT Fluorescent Oligo (44–2926, Thermo Fisher Scientific) was used as a scrambled non-targeting RNA control. Cells were incubated in the transfection mixture for 6 hr. Then, cells were washed with PBS and incubated in the maintenance medium overnight. Cells in the control wells were checked under the microscope for fluorescence the next day. Forty-eight hr post-treatment, cells were washed with PBS, trypsinized (0.05% Trypsin-EDTA; 15400–054, Thermo Fisher Scientific) and total RNA was extracted using RNeasy Plus Mini Kit (74134, QIAGEN) following the manufacturer's protocol. The knockdown experiment was done in three biological replicates. To test for the efficiency of the knockdown, cDNA was synthesized from 100 to 200 ng RNA using Maxima H Minus First Strand cDNA Synthesis Kit (K1652, Thermo Fisher Scientific) following the manufacturer's protocol. qRT-PCR was performed using QuantiTect SYBR Green PCR (204143, QIAGEN). *HAND2* primers: forward CACCAGCTACATCGCC TACC, reverse ATTTCGTTCAGCTCCTTCTTCC. *GAPDH* housekeeping gene was used for normalization; primers forward AATCCCATCACCATCTTCCA, reverse TGGACTCCACGACGTACTCA. Samples that showed >70% knockdown efficiency were used for RNA-Seq.

HAND2 knockdown RNA-Seq analysis

RNA from knockdown and control samples were DNase treated with TURBO DNA-free Kit (AM1907, Thermo Fisher Scientific) and RNA quality and quantity were assessed on 2100 Bioanalyzer (Agilent Technologies, Inc). RNA-Seq libraries were prepared using TruSeq Stranded Total RNA Library Prep Kit with Ribo-Zero Human (RS-122–2201, Illumina Inc) following manufacturer's protocol. Library quality and quantity were checked on 2100 Bioanalyzer and the pool of libraries was sequenced on Illumina HiSEQ4000 (single-end 50 bp) using manufacturer's reagents and protocols. Quality control, Ribo-Zero library preparation and Illumina sequencing were performed at the Genomics Facility at The University of Chicago.

All sequencing data were uploaded and analyzed on the Galaxy platform (https://usegalaxy.org/; Version 20.01). Individual reads for particular samples were concatenated using the 'Concatenate datasets' tool (version 1.0.0). We used HISAT2 (version 2.1.0+galaxy5) (*Kim et al., 2015*) to align reads to the Human hg38 reference genome using 'Single-end' option, and reporting alignments tailored for transcript assemblers including StringTie. Transcripts were assembled and quantified using StringTie (v1.3.6) (*Pertea et al., 2015*; *Pertea et al., 2016*), with reference file to guide assembly and the 'reference transcripts only' option, and output count files for differential expression with DESeq2/edgeR/limma-voom. Differentially expressed genes were identified using DESeq2 (version 2.11.40.6+galaxy1; *Anders and Huber, 2010*; *Love et al., 2014*). The reference file for StringTie guided assembly was wgEncodeGencodeBasicV33. The volcano plot was generated using *Blighe et al., 2020*.

Trans-well migration assay

Human hTERT-immortalized ESFs (CRL-4003, ATCC) were selected as a model ESF cell line because they are proliferative, maintain hormone responsiveness, and gene expression patterns characteristic of primary ESFs, and have been relatively well characterized (*Krikun et al., 2004*). ESFs were cultured in the maintenance medium as described above in T75 flasks until ~80% confluent. Cryopreserved primary adult human CD56+ NK cells purified by immunomagnetic bead separation were obtained from ATCC (PCS-800–019) and cultured in RPMI-1640 containing 10% FBS and 500 IU/ml IL2 in T75 flasks for 2 days prior to trans-well migration assays. We used the immortalized first trimester extravillous trophoblast cell line HTR-8/SVneo (*Graham et al., 1993*), because it maintains characteristics of extravillous trophoblasts and has previously been shown to be a good model of trophoblast migration and invasion (*Iacob et al., 2008*; *Paiva et al., 2009*; *Hannan et al., 2010*). HTR-8/SVneo cells were obtained from ATCC (CRL-3271) and cultured in RPMI-1640 containing 5%

FBS in T75 flasks for 2 days prior to trans-well migration assays. All cell lines were determined to be mycoplasma free before each experiment.

A total of 3×10^4 ESFs were plated per well of a 24-well plate and 18 hr later cells were transfected in Opti-MEM with 10 nM (per well) of siRNA targeting *HAND2* (s18133; Silencer Select Pre-Designed siRNA, cat # 4392420; Thermo Fisher Scientific) or *IL15* (s7377; Silencer Select Pre-Designed siRNA, cat # 4392420; Thermo Fisher Scientific) and 1.5 µl (per well) of Lipofectamine RNAiMAX (133778–150; Invitrogen). As a negative control we used Silencer Select negative control No. 1 (4390843; Thermo Fisher Scientific). ESFs were incubated in the transfection mixture for 6 hr. Then, ESFs were washed with warm PBS and incubated in the maintenance medium overnight. Efficiency of the knockdown was confirmed 48 hr post-treatment by qRT-PCR, media from each well was transferred to new 24-well plates and stored at 4°C. Total RNA from cells was extracted using RNeasy Plus Mini Kit (74134, QIAGEN) following the manufacturer's protocol. cDNA was synthesized from 10 ng RNA using Maxima H Minus First Strand cDNA Synthesis Kit (K1652, Thermo Fisher Scientific) following the manufacturer's protocol. qRT-PCR was performed using TaqMan Fast Universal PCR Master Mix 2X (4352042, Thermo Fisher Scientific), with primers for *HAND2* (Hs00232769_m1), *IL15* (Hs01003716_m1), and *Malat* (Hs00273907_s1) as a control housekeeping gene. Conditioned media from samples with >70% knockdown efficiency was used for trans-well migration assays.

Corning HTS Trans-well permeable supports were used for the trans-well migration assay (Corning, cat # CLS3398). Prior to the assays, 500 µl of media conditioned for 12 hr was centrifuged for 3 min at 1000 RPM to pellet any cells. For experiments using recombinant human IL15 (rhIL15), we added 10 ng/ml (AbCam, ab259403) of rhIL15 to fresh, non-conditioned ESF media; 10 ng/ml has previously been shown to induce migration of JEG-3 choriocarcinoma cells (*Zygmunt et al., 1998*). For neutralizing antibody experiments, either 1 µg/ml of anti-IL15 IgG (AbCam cat # MA5-23729) or control IgG (AbCam cat # 31903) were added to non-conditioned ESF media; 1 µg/ml has previously been shown to neutralize ESF-derived proteins and inhibit AC-1M88 trophoblast cell migration in trans-well assays (*Gellersen et al., 2010*; *Gellersen et al., 2013*). Plates were incubated with shaking at 37°C for 30 min prior to initiation of migration assays. During antibody incubation, NK and HTR-8/SVneo cells were collected and resuspended in fresh ESF growth media. For the trans-well migration assay, 5×10^6 of either NK or HTR-8/SVneo cells were added to each well of the upper chamber and either treatment or control media were added to the lower chambers. Plates were incubated at 37°C with 5% CO_2.

After 8 hr incubation, we removed the upper plate (containing remaining NK and HTR-8/SVneo cells) and discarded non-migrated cells. Fifty µl from each well in the lower chamber was transferred into a single well of a 96-well opaque plate. We used the CellTiter-Glo luminescent cell viability assay (G7570, Promega) to measure luminescence, which is proportional to the number of live cells per well. Data are reported as effect sizes (mean differences) between treatment and control. Confidence intervals are bias-corrected and accelerated. The p-values reported are the likelihoods of the observed effect sizes, if the null hypothesis of zero difference is true and calculated from a two-sided permutation t-test (5000 reshuffles of the control and test labels). Cumming estimation plots and estimation statistics were calculated using DABEST R package (*Ho et al., 2019*).

Acknowledgements

Additional information

Author contributions

Mirna Marinić, Conceptualization, Data curation, Formal analysis, Investigation, Writing - original draft, Writing - review and editing; Katelyn Mika, Conceptualization, Data curation, Formal analysis, Methodology, Writing - original draft, Writing - review and editing; Sravanthi Chigurupati, Formal analysis, Writing - original draft; Vincent J Lynch, Conceptualization, Data curation, Formal analysis, Supervision, Funding acquisition, Investigation, Visualization, Writing - original draft, Project administration, Writing - review and editing

Author ORCIDs

Mirna Marinić (iD) https://orcid.org/0000-0002-7037-8389
Katelyn Mika (iD) https://orcid.org/0000-0002-2170-9364
Vincent J Lynch (iD) https://orcid.org/0000-0001-5311-3824

Decision letter and Author response

Decision letter https://doi.org/10.7554/eLife.61257.sa1
Author response https://doi.org/10.7554/eLife.61257.sa2

Additional files

Supplementary files

• Transparent reporting form

Data availability

Sequencing data have been deposited in GEO under accession codes GSE155170 and GSE155322.

The following datasets were generated:

Author(s)	Year	Dataset title	Dataset URL	Database and Identifier
Mika K, Lynch VJ	2021	Mouse Endometrium Individual 1	https://www.ncbi.nlm.nih.gov/geo/query/acc.cgi?acc=GSM5100045	NCBI Gene Expression Omnibus, GSM5100045
Mika K, Lynch VJ	2021	Mouse Endometrium Individual 2	https://www.ncbi.nlm.nih.gov/geo/query/acc.cgi?acc=GSM5100046	NCBI Gene Expression Omnibus, GSM5100046
Mika K, Lynch VJ	2021	Mouse Endometrium Individual 3	https://www.ncbi.nlm.nih.gov/geo/query/acc.cgi?acc=GSM5100047	NCBI Gene Expression Omnibus , GSM5100047
Mika K, Lynch VJ	2020	Baboon Endometrium Individual 1	https://www.ncbi.nlm.nih.gov/geo/query/acc.cgi?acc=GSM4696515	NCBI Gene Expression Omnibus, GSM4696515
Mika K, Lynch VJ	2020	Baboon Endometrium Individual 2	https://www.ncbi.nlm.nih.gov/geo/query/acc.cgi?acc=GGSM4696516	NCBI Gene Expression Omnibus, GGSM4696516

Mika K, Lynch VJ	2020	Baboon Endometrium Individual 3	https://www.ncbi.nlm.nih.gov/geo/query/acc.cgi?acc=GSM4696517	NCBI Gene Expression Omnibus, GSM4696517
Mika K, Lynch VJ	2020	Hamster Endometrium Individual 1 Replicate 1	https://www.ncbi.nlm.nih.gov/geo/query/acc.cgi?acc=GSM4696518	NCBI Gene Expression Omnibus, GSM4696518
Mika K, Lynch VJ	2020	Hamster Endometrium Individual 2 Replicate 1	https://www.ncbi.nlm.nih.gov/geo/query/acc.cgi?acc=GSM4696519	NCBI Gene Expression Omnibus, GSM4696519
Mika K, Lynch VJ	2020	Hamster Endometrium Individual 3 Replicate 1	https://www.ncbi.nlm.nih.gov/geo/query/acc.cgi?acc=GSM4696520	NCBI Gene Expression Omnibus, GSM4696520
Mika K, Lynch VJ	2020	Hamster Endometrium Individual 1 Replicate 2	https://www.ncbi.nlm.nih.gov/geo/query/acc.cgi?acc=GSM4696521	NCBI Gene Expression Omnibus, GSM4696521
Mika K, Lynch VJ	2020	Hamster Endometrium Individual 2 Replicate 2	https://www.ncbi.nlm.nih.gov/geo/query/acc.cgi?acc=GSM4696522	NCBI Gene Expression Omnibus, GSM4696522
Mika K, Lynch VJ	2020	Hamster Endometrium Individual 3 Replicate 2	https://www.ncbi.nlm.nih.gov/geo/query/acc.cgi?acc=GSM4696523	NCBI Gene Expression Omnibus, GSM4696523
Mika K, Lynch VJ	2020	Bat Endometrium Individual 1	https://www.ncbi.nlm.nih.gov/geo/query/acc.cgi?acc=GSM4696524	NCBI Gene Expression Omnibus, GSM4696524
Mika K, Lynch VJ	2020	Bat Endometrium Individual 2	https://www.ncbi.nlm.nih.gov/geo/query/acc.cgi?acc=GSM4696525	NCBI Gene Expression Omnibus, GSM4696525
Mika K, Lynch VJ	2020	Squirrel Endometrium Individual 1	https://www.ncbi.nlm.nih.gov/geo/query/acc.cgi?acc=GSM4696526	NCBI Gene Expression Omnibus, GSM4696526
Mika K, Lynch VJ	2020	Squirrel Endometrium Individual 2	https://www.ncbi.nlm.nih.gov/geo/query/acc.cgi?acc=GSM4696527	NCBI Gene Expression Omnibus, GSM4696527
Marinić M, Lynch VJ	2020	siRNA Ctrl_rep1a	https://www.ncbi.nlm.nih.gov/geo/query/acc.cgi?acc=GSM4699113	NCBI Gene Expression Omnibus, GSM4699113
Marinić M, Lynch VJ	2020	siRNA Ctrl_rep1b	https://www.ncbi.nlm.nih.gov/geo/query/acc.cgi?acc=GSM4699114	NCBI Gene Expression Omnibus, GSM4699114
Marinić M, Lynch VJ	2020	siRNA Ctrl_rep2a	https://www.ncbi.nlm.nih.gov/geo/query/acc.cgi?acc=GSM4699115	NCBI Gene Expression Omnibus, GSM4699115
Marinić M, Lynch VJ	2020	siRNA Ctrl_rep2b	https://www.ncbi.nlm.nih.gov/geo/query/acc.cgi?acc=GSM4699116	NCBI Gene Expression Omnibus, GSM4699116
Marinić M, Lynch VJ	2020	siRNA Ctrl_rep3a	https://www.ncbi.nlm.nih.gov/geo/query/acc.cgi?acc=GSM4699117	NCBI Gene Expression Omnibus, GSM4699117
Marinić M, Lynch VJ	2020	siRNA Ctrl_rep3b	https://www.ncbi.nlm.nih.gov/geo/query/acc.cgi?acc=GSM4699118	NCBI Gene Expression Omnibus, GSM4699118
Marinić M, Lynch VJ	2020	siRNA HAND2_rep1a	https://www.ncbi.nlm.nih.gov/geo/query/acc.cgi?acc=GSM4699119	NCBI Gene Expression Omnibus, GSM4699119
Marinić M, Lynch VJ	2020	siRNA HAND2_rep1b	https://www.ncbi.nlm.nih.gov/geo/query/acc.cgi?acc=GSM4699120	NCBI Gene Expression Omnibus, GSM4699120
Marinić M, Lynch VJ	2020	siRNA HAND2_rep2a	https://www.ncbi.nlm.nih.gov/geo/query/acc.cgi?acc=GSM4699121	NCBI Gene Expression Omnibus, GSM4699121
Marinić M, Lynch VJ	2020	siRNA HAND2_rep2b	https://www.ncbi.nlm.nih.gov/geo/query/acc.	NCBI Gene Expression Omnibus, GSM4699122

			cgi?acc=GSM4699122	
Marinić M, Lynch VJ	2020	siRNA HAND2_rep3a	https://www.ncbi.nlm.nih.gov/geo/query/acc.cgi?acc=GSM4699123	NCBI Gene Expression Omnibus, GSM4699123
Marinić M, Lynch VJ	2020	siRNA HAND2_rep3b	https://www.ncbi.nlm.nih.gov/geo/query/acc.cgi?acc=GSM4699124	NCBI Gene Expression Omnibus, GSM4699124
Mika K, Lynch VJ	2020	Evolutionary transcriptomics implicates HAND2 in the origins of implantation and regulation of gestation length	https://www.ncbi.nlm.nih.gov/geo/query/acc.cgi?acc=GSE155170	NCBI Gene Expression Omnibus, GSE155170
Marinić M, Lynch VJ	2020	Evolutionary transcriptomics implicates HAND2 in the origins of implantation and regulation of gestation length	https://www.ncbi.nlm.nih.gov/geo/query/acc.cgi?acc=GSE155322	NCBI Gene Expression Omnibus, GSE155322

References

Abbott BD, Schmid JE, Pitt JA, Buckalew AR, Wood CR, Held GA, Diliberto JJ. 1999. Adverse reproductive outcomes in the transgenic Ah receptor-deficient mouse. *Toxicology and Applied Pharmacology* **155**:62–70. DOI: https://doi.org/10.1006/taap.1998.8601, PMID: 10036219

Abegglen LM, Caulin AF, Chan A, Lee K, Robinson R, Campbell MS, Kiso WK, Schmitt DL, Waddell PJ, Bhaskara S, Jensen ST, Maley CC, Schiffman JD. 2015. Potential mechanisms for cancer resistance in elephants and comparative cellular response to DNA damage in humans. *Jama* **314**:1850–1860. DOI: https://doi.org/10.1001/jama.2015.13134, PMID: 26447779

Afgan E, Baker D, Batut B, van den Beek M, Bouvier D, Cech M, Chilton J, Clements D, Coraor N, Grüning BA, Guerler A, Hillman-Jackson J, Hiltemann S, Jalili V, Rasche H, Soranzo N, Goecks J, Taylor J, Nekrutenko A, Blankenberg D. 2018. The Galaxy platform for accessible, reproducible and collaborative biomedical analyses: 2018 update. *Nucleic Acids Research* **46**:W537–W544. DOI: https://doi.org/10.1093/nar/gky379, PMID: 29790989

Allavena P, Giardina G, Bianchi G, Mantovani A. 1997. IL-15 is chemotactic for natural killer cells and stimulates their adhesion to vascular endothelium. *Journal of Leukocyte Biology* **61**:729–735. DOI: https://doi.org/10.1002/jlb.61.6.729

Allport VC, Pieber D, Slater DM, Newton R, White JO, Bennett PR. 2001. Human labour is associated with nuclear factor-kappaB activity which mediates cyclo-oxygenase-2 expression and is involved with the 'functional progesterone withdrawal'. *Molecular Human Reproduction* **7**:581–586. DOI: https://doi.org/10.1093/molehr/7.6.581, PMID: 11385114

Anders S, Huber W. 2010. Differential expression analysis for sequence count data. *Genome Biology* **11**:r106. DOI: https://doi.org/10.1186/gb-2010-11-10-r106, PMID: 20979621

Armstrong DL, McGowen MR, Weckle A, Pantham P, Caravas J, Agnew D, Benirschke K, Savage-Rumbaugh S, Nevo E, Kim CJ, Wagner GP, Romero R, Wildman DE. 2017. The core transcriptome of mammalian placentas and the divergence of expression with placental shape. *Placenta* **57**:71–78. DOI: https://doi.org/10.1016/j.placenta.2017.04.015, PMID: 28864021

Arthur A. 2018. Molecular evolution of genes associated with preeclampsia: genetic conflict, antagonistic coevolution and signals of selection'. *Journal of Evolutionary Medicine* **6**:msq034. DOI: https://doi.org/10.1093/molbev/msq034

Ashkar AA, Black GP, Wei Q, He H, Liang L, Head JR, Croy BA. 2003. Assessment of requirements for IL-15 and IFN regulatory factors in uterine NK cell differentiation and function during pregnancy. *The Journal of Immunology* **171**:2937–2944. DOI: https://doi.org/10.4049/jimmunol.171.6.2937, PMID: 12960317

Bany BM, Scott CA, Eckstrum KS. 2012. Analysis of uterine gene expression in interleukin-15 knockout mice reveals uterine natural killer cells do not play a major role in decidualization and associated angiogenesis. *Reproduction* **143**:359–375. DOI: https://doi.org/10.1530/REP-11-0325, PMID: 22187674

Barber EM, Pollard JW. 2003. The uterine NK cell population requires IL-15 but these cells are not required for pregnancy nor the resolution of a Listeria monocytogenes infection. *The Journal of Immunology* **171**:37–46. DOI: https://doi.org/10.4049/jimmunol.171.1.37, PMID: 12816981

Bartmann C, Segerer SE, Rieger L, Kapp M, Sütterlin M, Kämmerer U. 2014. Quantification of the predominant immune cell populations in decidua throughout human pregnancy. *American Journal of Reproductive Immunology* **71**:109–119. DOI: https://doi.org/10.1111/aji.12185, PMID: 24330065

Blighe K, Rana S, Lewis M. 2020. EnhancedVolcano: Publication-ready volcano plots with enhanced coloring and labeling. *EnhancedVolcano.* R package version 1.8.0. https://github.com/kevinblighe/EnhancedVolcano

Boretto M, Cox B, Noben M, Hendriks N, Fassbender A, Roose H, Amant F, Timmerman D, Tomassetti C, Vanhie A, Meuleman C, Ferrante M, Vankelecom H. 2017. Development of organoids from mouse and human endometrium showing endometrial epithelium physiology and long-term expandability. *Development* **144**:1775–1786. DOI: https://doi.org/10.1242/dev.148478, PMID: 28442471

Bray NL, Pimentel H, Melsted P, Pachter L. 2016. Near-optimal probabilistic RNA-seq quantification. *Nature Biotechnology* **34**:525–527. DOI: https://doi.org/10.1038/nbt.3519

Brayer KJ, Lynch VJ, Wagner GP. 2011. Evolution of a derived protein-protein interaction between HoxA11 and Foxo1a in mammals caused by changes in intramolecular regulation. *PNAS* **108**:E414–E420. DOI: https://doi.org/10.1073/pnas.1100990108, PMID: 21788518

Brighton PJ, Maruyama Y, Fishwick K, Vrljicak P, Tewary S, Fujihara R, Muter J, Lucas ES, Yamada T, Woods L, Lucciola R, Hou Lee Y, Takeda S, Ott S, Hemberger M, Quenby S, Brosens JJ. 2017. Clearance of senescent decidual cells by uterine natural killer cells in cycling human endometrium. *eLife* **6**:e31274. DOI: https://doi.org/10.7554/eLife.31274, PMID: 29227245

Brockway HM, Kallapur SG, Buhimschi IA, Buhimschi CS, Ackerman WE, Muglia LJ, Jones HN. 2019. Unique transcriptomic landscapes identified in idiopathic spontaneous and infection related preterm births compared to normal term births. *PLOS ONE* **14**:e0225062. DOI: https://doi.org/10.1371/journal.pone.0225062, PMID: 31703110

Bulmer JN, Morrison L, Longfellow M, Ritson A, Pace D. 1991. Granulated lymphocytes in human endometrium: histochemical and immunohistochemical studies. *Human Reproduction* **6**:791–798. DOI: https://doi.org/10.1093/oxfordjournals.humrep.a137430, PMID: 1757516

Burke SD, Barrette VF, Gravel J, Carter AL, Hatta K, Zhang J, Chen Z, Leno-Durán E, Bianco J, Leonard S, Murrant C, Adams MA, Croy BA. 2010. Uterine NK cells, spiral artery modification and the regulation of blood pressure during mouse pregnancy. *American Journal of Reproductive Immunology* **63**:472–481. DOI: https://doi.org/10.1111/j.1600-0897.2010.00818.x, PMID: 20175772

Buzzio OL, Lu Z, Miller CD, Unterman TG, Kim JJ. 2006. FOXO1A differentially regulates genes of decidualization. *Endocrinology* **147**:3870–3876. DOI: https://doi.org/10.1210/en.2006-0167, PMID: 16690806

Chekir C, Nakatsuka M, Noguchi S, Konishi H, Kamada Y, Sasaki A, Hao L, Hiramatsu Y. 2006. Accumulation of advanced glycation end products in women with preeclampsia: possible involvement of placental oxidative and nitrative stress. *Placenta* **27**:225–233. DOI: https://doi.org/10.1016/j.placenta.2005.02.016, PMID: 16338468

Chen Y, Zhuang Y, Chen X, Huang L. 2011. Effect of human endometrial stromal cell-derived conditioned medium on uterine natural killer (uNK) cells' proliferation and cytotoxicity. *American Journal of Reproductive Immunology* **65**:589–596. DOI: https://doi.org/10.1111/j.1600-0897.2010.00955.x, PMID: 21223424

Curlewis JD, Stone GM. 1987. Effects of oestradiol, the oestrous cycle and pregnancy on weight, metabolism and cytosol receptors in the oviduct and vaginal complex of the brushtail possum (*Trichosurus vulpecula*). *Australian Journal of Biological Sciences* **40**:315–322. DOI: https://doi.org/10.1071/BI9870315, PMID: 3442515

Davis S, Meltzer PS. 2007. GEOquery: a bridge between the gene expression omnibus (GEO) and BioConductor. *Bioinformatics* **23**:1846–1847. DOI: https://doi.org/10.1093/bioinformatics/btm254, PMID: 17496320

Dunn CL, Critchley HO, Kelly RW. 2002. IL-15 regulation in human endometrial stromal cells. *The Journal of Clinical Endocrinology & Metabolism* **87**:1898–1901. DOI: https://doi.org/10.1210/jcem.87.4.8539, PMID: 11932337

Eidem HR, Rinker DC, Ackerman WE, Buhimschi IA, Buhimschi CS, Dunn-Fletcher C, Kallapur SG, Pavličev M, Muglia LJ, Abbot P, Rokas A. 2016. Comparing human and macaque placental transcriptomes to disentangle preterm birth pathology from gestational age effects. *Placenta* **41**:74–82. DOI: https://doi.org/10.1016/j.placenta.2016.03.006, PMID: 27208410

Elliot MG. 2017. Evolutionary origins of preeclampsia. *Pregnancy Hypertension: An International Journal of Women's Cardiovascular Health* **7**:56. DOI: https://doi.org/10.1016/j.preghy.2016.10.006

Erlebacher A. 2013. Mechanisms of T cell tolerance towards the allogeneic fetus. *Nature Reviews Immunology* **13**:23–33. DOI: https://doi.org/10.1038/nri3361, PMID: 23237963

Felker AM, Croy BA. 2016. Uterine natural killer cell partnerships in early mouse decidua basalis. *Journal of Leukocyte Biology* **100**:645–655. DOI: https://doi.org/10.1189/jlb.1HI0515-226R, PMID: 27001968

Feng J, Liu T, Qin B, Zhang Y, Liu XS. 2012. Identifying ChIP-seq enrichment using MACS. *Nature Protocols* **7**:1728–1740. DOI: https://doi.org/10.1038/nprot.2012.101, PMID: 22936215

Franco HL, Dai D, Lee KY, Rubel CA, Roop D, Boerboom D, Jeong JW, Lydon JP, Bagchi IC, Bagchi MK, DeMayo FJ. 2011. WNT4 is a key regulator of normal postnatal uterine development and progesterone signaling during embryo implantation and decidualization in the mouse. *The FASEB Journal* **25**:1176–1187. DOI: https://doi.org/10.1096/fj.10-175349, PMID: 21163860

Fraser R, Whitley GS, Thilaganathan B, Cartwright JE. 2015. Decidual natural killer cells regulate vessel stability: implications for impaired spiral artery remodelling. *Journal of Reproductive Immunology* **110**:54–60. DOI: https://doi.org/10.1016/j.jri.2015.04.003, PMID: 26004035

Fukuda T, Shirane A, Wada-Hiraike O, Oda K, Tanikawa M, Sakuabashi A, Hirano M, Fu H, Morita Y, Miyamoto Y, Inaba K, Kawana K, Osuga Y, Fujii T. 2015. HAND2-mediated proteolysis negatively regulates the function of estrogen receptor α. *Molecular Medicine Reports* **12**:5538–5544. DOI: https://doi.org/10.3892/mmr.2015.4070, PMID: 26166202

Funeshima N, Fujino M, Kitazawa Y, Hara Y, Hara Y, Hayakawa K, Okuyama T, Kimura H, Li XK. 2005. Inhibition of allogeneic T-cell responses by dendritic cells expressing transduced indoleamine 2,3-dioxygenase. *The Journal of Gene Medicine* **7**:565–575. DOI: https://doi.org/10.1002/jgm.698, PMID: 15543532

Garrido-Gomez T, Dominguez F, Quiñonero A, Diaz-Gimeno P, Kapidzic M, Gormley M, Ona K, Padilla-Iserte P, McMaster M, Genbacev O, Perales A, Fisher SJ, Simón C. 2017. Defective decidualization during and after severe preeclampsia reveals a possible maternal contribution to the etiology. *PNAS* **114**:E8468–E8477. DOI: https://doi.org/10.1073/pnas.1706546114, PMID: 28923940

Gellersen B, Reimann K, Samalecos A, Aupers S, Bamberger AM. 2010. Invasiveness of human endometrial stromal cells is promoted by decidualization and by trophoblast-derived signals. *Human Reproduction* **25**:862–873. DOI: https://doi.org/10.1093/humrep/dep468, PMID: 20118488

Gellersen B, Wolf A, Kruse M, Schwenke M, Bamberger A-M. 2013. Human endometrial stromal cell-trophoblast interactions: mutual stimulation of chemotactic migration and promigratory roles of cell surface molecules CD82 and CEACAM11. *Biology of Reproduction* **88**:106724. DOI: https://doi.org/10.1095/biolreprod.112.106724

Gellersen B, Brosens J. 2003. Cyclic AMP and progesterone receptor cross-talk in human endometrium: a decidualizing affair. *Journal of Endocrinology* **178**:357–372. DOI: https://doi.org/10.1677/joe.0.1780357

Gentleman RC, Carey VJ, Bates DM, Bolstad B, Dettling M, Dudoit S, Ellis B, Gautier L, Ge Y, Gentry J, Hornik K, Hothorn T, Huber W, Iacus S, Irizarry R, Leisch F, Li C, Maechler M, Rossini AJ, Sawitzki G, et al. 2004. Bioconductor: open software development for computational biology and bioinformatics. *Genome Biology* **5**:r80. DOI: https://doi.org/10.1186/gb-2004-5-10-r80, PMID: 15461798

Girling JE. 2002. The reptilian oviduct: a review of structure and function and directions for future research. *Journal of Experimental Zoology* **293**:141–170. DOI: https://doi.org/10.1002/jez.10105

Godbole G, Suman P, Gupta SK, Modi D. 2011. Decidualized endometrial stromal cell derived factors promote trophoblast invasion. *Fertility and Sterility* **95**:1278–1283. DOI: https://doi.org/10.1016/j.fertnstert.2010.09.045, PMID: 21067732

Godbole G, Modi D. 2010. Regulation of decidualization, interleukin-11 and interleukin-15 by homeobox A 10 in endometrial stromal cells. *Journal of Reproductive Immunology* **85**:130–139. DOI: https://doi.org/10.1016/j.jri.2010.03.003, PMID: 20478621

Gomaa MF, Serag Eldeen IF, Farid LA, El-Saeed MME, Abas AM, Aawd NM. 2017. Uterine natural killer cells dysregulation in idiopathic human preterm birth: a pilot study. *The Journal of Maternal-Fetal & Neonatal Medicine* **30**:1782–1786. DOI: https://doi.org/10.1080/14767058.2016.1224840, PMID: 27593347

Gomez-Lopez N, Guilbert LJ, Olson DM. 2010. Invasion of the leukocytes into the fetal-maternal interface during pregnancy. *Journal of Leukocyte Biology* **88**:625–633. DOI: https://doi.org/10.1189/jlb.1209796, PMID: 2051 9637

González-Morán MG. 2015. Immunohistochemical localization of progesterone receptor isoforms and estrogen receptor alpha in the chicken oviduct magnum during development. *Acta Histochemica* **117**:681–687. DOI: https://doi.org/10.1016/j.acthis.2015.10.003, PMID: 26519127

Graham CH, Hawley TS, Hawley RG, MacDougall JR, Kerbel RS, Khoo N, Lala PK. 1993. Establishment and characterization of first trimester human trophoblast cells with extended lifespan. *Experimental Cell Research* **206**:204–211. DOI: https://doi.org/10.1006/excr.1993.1139, PMID: 7684692

Graham CH, Lala PK. 1991. Mechanism of control of trophoblast invasion in situ. *Journal of Cellular Physiology* **148**:228–234. DOI: https://doi.org/10.1002/jcp.1041480207, PMID: 1652588

Greenhill C. 2014. Reproductive endocrinology: circadian clock involved in embryo implantation. *Nature Reviews. Endocrinology* **10**:701. DOI: https://doi.org/10.1038/nrendo.2014.174, PMID: 25287286

Griffith OW, Chavan AR, Protopapas S, Maziarz J, Romero R, Wagner GP. 2017. Embryo implantation evolved from an ancestral inflammatory attachment reaction. *PNAS* **114**:E6566–E6575. DOI: https://doi.org/10.1073/pnas.1701129114, PMID: 28747528

Griffith OW, Chavan AR, Pavlicev M, Protopapas S, Callahan R, Maziarz J, Wagner GP. 2019. Endometrial recognition of pregnancy occurs in the grey short-tailed opossum (*Monodelphis domestica*). *Proceedings of the Royal Society B: Biological Sciences* **286**:20190691. DOI: https://doi.org/10.1098/rspb.2019.0691

Guedes-Martins L, Matos L, Soares A, Silva E, Almeida H. 2013. AGEs, contributors to placental bed vascular changes leading to preeclampsia. *Free Radical Research* **47**:70–80. DOI: https://doi.org/10.3109/10715762.2013.815347, PMID: 23796030

Guleria I, Pollard JW. 2000. The trophoblast is a component of the innate immune system during pregnancy. *Nature Medicine* **6**:589–593. DOI: https://doi.org/10.1038/75074, PMID: 10802718

Hamilton S, Oomomian Y, Stephen G, Shynlova O, Tower CL, Garrod A, Lye SJ, Jones RL. 2012. Macrophages infiltrate the human and rat decidua during term and preterm labor: evidence that decidual inflammation precedes labor. *Biology of Reproduction* **86**:095505. DOI: https://doi.org/10.1095/biolreprod.111.095505

Hanna J, Goldman-Wohl D, Hamani Y, Avraham I, Greenfield C, Natanson-Yaron S, Prus D, Cohen-Daniel L, Arnon TI, Manaster I, Gazit R, Yutkin V, Benharroch D, Porgador A, Keshet E, Yagel S, Mandelboim O. 2006. Decidual NK cells regulate key developmental processes at the human fetal-maternal interface. *Nature Medicine* **12**:1065–1074. DOI: https://doi.org/10.1038/nm1452, PMID: 16892062

Hannan NJ, Paiva P, Dimitriadis E, Salamonsen LA. 2010. Models for study of human embryo implantation: choice of cell lines? *Biology of Reproduction* **82**:235–245. DOI: https://doi.org/10.1095/biolreprod.109.077800, PMID: 19571263

Hansen VL, Schilkey FD, Miller RD. 2016. Transcriptomic changes associated with pregnancy in a marsupial, the gray short-tailed opossum *Monodelphis domestica*. *PLOS ONE* **11**:e0161608. DOI: https://doi.org/10.1371/journal.pone.0161608, PMID: 27598793

Hao K, Zhou Q, Chen W, Jia W, Zheng J, Kang J, Wang K, Duan T. 2013. Possible role of the 'IDO-AhR axis' in maternal-foetal tolerance. *Cell Biology International* **37**:105–108. DOI: https://doi.org/10.1002/cbin.10023, PMID: 23319400

Hayashi K, Erikson DW, Tilford SA, Bany BM, Maclean JA, Rucker EB, Johnson GA, Spencer TE. 2009. Wnt genes in the mouse uterus: potential regulation of implantation. *Biology of Reproduction* **80**:989–1000. DOI: https://doi.org/10.1095/biolreprod.108.075416, PMID: 19164167

Hazan AD, Smith SD, Jones RL, Whittle W, Lye SJ, Dunk CE. 2010. Vascular-leukocyte interactions: mechanisms of human decidual spiral artery remodeling in vitro. *American Journal of Pathology* **177**:1017–1030. DOI: https://doi.org/10.2353/ajpath.2010.091105

Hiby SE, Apps R, Sharkey AM, Farrell LE, Gardner L, Mulder A, Claas FH, Walker JJ, Redman CC, Morgan L, Tower C, Regan L, Moore GE, Carrington M, Moffett A. 2010. Maternal activating KIRs protect against human reproductive failure mediated by fetal HLA-C2. *Journal of Clinical Investigation* **120**:4102–4110. DOI: https://doi.org/10.1172/JCI43998

Hill JP. 1936. The development of the Monotremata-*Part I The histology of the oviduct during gestation by Catherine J Hill BSc, PhD part II the structure of the Egg-shell. The Transactions of the Zoological Society of London* **21**:413–476. DOI: https://doi.org/10.1111/j.1096-3642.1936.tb00458.x

Ho J, Tumkaya T, Aryal S, Choi H, Claridge-Chang A. 2019. Moving beyond P values: data analysis with estimation graphics. *Nature Methods* **16**:565–566. DOI: https://doi.org/10.1038/s41592-019-0470-3, PMID: 31217592

Hou ZC, Sterner KN, Romero R, Than NG, Gonzalez JM, Weckle A, Xing J, Benirschke K, Goodman M, Wildman DE. 2012. Elephant transcriptome provides insights into the evolution of eutherian placentation. *Genome Biology and Evolution* **4**:713–725. DOI: https://doi.org/10.1093/gbe/evs045, PMID: 22546564

Huyen DV, Bany BM. 2011. Evidence for a conserved function of heart and neural crest derivatives expressed transcript 2 in mouse and human decidualization. *Reproduction* **142**:353–368. DOI: https://doi.org/10.1530/REP-11-0060, PMID: 21527398

Iacob D, Cai J, Tsonis M, Babwah A, Chakraborty C, Bhattacharjee RN, Lala PK. 2008. Decorin-mediated inhibition of proliferation and migration of the human trophoblast via different tyrosine kinase receptors. *Endocrinology* **149**:6187–6197. DOI: https://doi.org/10.1210/en.2008-0780, PMID: 18703624

Jones RL, Stoikos C, Findlay JK, Salamonsen LA. 2006. TGF-β superfamily expression and actions in the endometrium and placenta. *Reproduction* **132**:217–232. DOI: https://doi.org/10.1530/rep.1.01076

Jones A, Teschendorff AE, Li Q, Hayward JD, Kannan A, Mould T, West J, Zikan M, Cibula D, Fiegl H, Lee SH, Wik E, Hadwin R, Arora R, Lemech C, Turunen H, Pakarinen P, Jacobs IJ, Salvesen HB, Bagchi MK, et al. 2013. Role of DNA methylation and epigenetic silencing of HAND2 in endometrial cancer development. *PLOS Medicine* **10**:e1001551. DOI: https://doi.org/10.1371/journal.pmed.1001551, PMID: 24265601

Kajihara T, Brosens JJ, Ishihara O. 2013. The role of FOXO1 in the decidual transformation of the endometrium and early pregnancy. *Medical Molecular Morphology* **46**:61–68. DOI: https://doi.org/10.1007/s00795-013-0018-z, PMID: 23381604

Kato S, Tora L, Yamauchi J, Masushige S, Bellard M, Chambon P. 1992. A far upstream estrogen response element of the ovalbumin gene contains several half-palindromic 5′-TGACC-3′ motifs acting synergistically. *Cell* **68**:731–742. DOI: https://doi.org/10.1016/0092-8674(92)90148-6, PMID: 1739978

Kato S, Endoh H, Masuhiro Y, Kitamoto T, Uchiyama S, Sasaki H, Masushige S, Gotoh Y, Nishida E, Kawashima H, Metzger D, Chambon P. 1995. Activation of the estrogen receptor through phosphorylation by mitogen-activated protein kinase. *Science* **270**:1491–1494. DOI: https://doi.org/10.1126/science.270.5241.1491, PMID: 7491495

Kieckbusch J, Gaynor LM, Moffett A, Colucci F. 2014. MHC-dependent inhibition of uterine NK cells impedes fetal growth and decidual vascular remodelling. *Nature Communications* **5**:4359. DOI: https://doi.org/10.1038/ncomms4359, PMID: 24577131

Kim JJ, Jaffe RC, Fazleabas AT. 1999. Blastocyst invasion and the stromal response in primates. *Human Reproduction* **14**:45–55. DOI: https://doi.org/10.1093/humrep/14.suppl_2.45, PMID: 10690800

Kim D, Langmead B, Salzberg SL. 2015. HISAT: a fast spliced aligner with low memory requirements. *Nature Methods* **12**:357–360. DOI: https://doi.org/10.1038/nmeth.3317, PMID: 25751142

King A, Balendran N, Wooding P, Carter NP, Loke YW. 1991. CD3- leukocytes present in the human uterus during early placentation: phenotypic and morphologic characterization of the CD56++ population. *Developmental Immunology* **1**:169–190. DOI: https://doi.org/10.1155/1991/83493, PMID: 1726555

Kitaya K, Yasuda J, Yagi I, Tada Y, Fushiki S, Honjo H. 2000. IL-15 expression at human endometrium and decidua. *Biology of Reproduction* **63**:683–687. DOI: https://doi.org/10.1095/biolreprod63.3.683, PMID: 10952908

Kitaya K, Yamaguchi T, Honjo H. 2005. Central role of interleukin-15 in postovulatory recruitment of peripheral blood CD16(-) natural killer cells into human endometrium. *The Journal of Clinical Endocrinology & Metabolism* **90**:2932–2940. DOI: https://doi.org/10.1210/jc.2004-2447, PMID: 15713701

Klonisch T, Wolf P, Hombach-Klonisch S, Vogt S, Kuechenhoff A, Tetens F, Fischer B. 2001. Epidermal growth factor-like ligands and erbB genes in the peri-implantation rabbit uterus and blastocyst. *Biology of Reproduction* **64**:1835–1844. DOI: https://doi.org/10.1095/biolreprod64.6.1835, PMID: 11369616

Kosova G, Stephenson MD, Lynch VJ, Ober C. 2015. Evolutionary forward genomics reveals novel insights into the genes and pathways dysregulated in recurrent early pregnancy loss. *Human Reproduction* **30**:519–529. DOI: https://doi.org/10.1093/humrep/deu355, PMID: 25586782

Krikun G, Mor G, Alvero A, Guller S, Schatz F, Sapi E, Rahman M, Caze R, Qumsiyeh M, Lockwood CJ. 2004. A novel immortalized human endometrial stromal cell line with normal progestational response. *Endocrinology* **145**:2291–2296. DOI: https://doi.org/10.1210/en.2003-1606, PMID: 14726435

LaBella AL. 2019. Accounting for diverse evolutionary forces reveals the mosaic nature of selection on genomic regions associated with human preterm birth. *bioRxiv*. DOI: https://doi.org/10.1101/816827

Lappas M, Permezel M, Rice GE. 2007. Advanced glycation endproducts mediate pro-inflammatory actions in human gestational tissues via nuclear factor-κB and extracellular signal-regulated kinase 1/2. *Journal of Endocrinology* **193**:269–277. DOI: https://doi.org/10.1677/JOE-06-0081

Large MJ, Wetendorf M, Lanz RB, Hartig SM, Creighton CJ, Mancini MA, Kovanci E, Lee KF, Threadgill DW, Lydon JP, Jeong JW, DeMayo FJ. 2014. The epidermal growth factor receptor critically regulates endometrial

function during early pregnancy. *PLOS Genetics* **10**:e1004451. DOI: https://doi.org/10.1371/journal.pgen.1004451, PMID: 24945252

Lash GE, Robson SC, Bulmer JN. 2010. Review: functional role of uterine natural killer (uNK) cells in human early pregnancy decidua. *Placenta* **31**:S87–S92. DOI: https://doi.org/10.1016/j.placenta.2009.12.022, PMID: 20061017

Laskarin G, Strbo N, Crncic TB, Juretic K, Bataille NL, Chaouat G, Rukavina D. 2006. Physiological role of IL-15 and IL-18 at the maternal-fetal interface. *Chemical Immunology and Allergy* **89**:10–25. DOI: https://doi.org/10.1159/000087906

Lédée N, Munaut C, Aubert J, Sérazin V, Rahmati M, Chaouat G, Sandra O, Foidart JM. 2011. Specific and extensive endometrial deregulation is present before conception in IVF/ICSI repeated implantation failures (IF) or recurrent miscarriages. *The Journal of Pathology* **225**:554–564. DOI: https://doi.org/10.1002/path.2948

Lee KY, Jeong JW, Wang J, Ma L, Martin JF, Tsai SY, Lydon JP, DeMayo FJ. 2007. Bmp2 is critical for the murine uterine decidual response. *Molecular and Cellular Biology* **27**:5468–5478. DOI: https://doi.org/10.1128/MCB.00342-07, PMID: 17515606

Li Q, Kannan A, Wang W, DeMayo FJ, Taylor RN, Bagchi MK, Bagchi IC. 2007. Bone morphogenetic protein 2 functions via a conserved signaling pathway involving Wnt4 to regulate uterine decidualization in the mouse and the human. *Journal of Biological Chemistry* **282**:31725–31732. DOI: https://doi.org/10.1074/jbc.M704723200

Li Q, Kannan A, DeMayo FJ, Lydon JP, Cooke PS, Yamagishi H, Srivastava D, Bagchi MK, Bagchi IC. 2011. The antiproliferative action of progesterone in uterine epithelium is mediated by Hand2. *Science* **331**:912–916. DOI: https://doi.org/10.1126/science.1197454, PMID: 21330545

Li Q. 2014. Transforming growth factor β signaling in uterine development and function. *Journal of Animal Science and Biotechnology* **5**:52. DOI: https://doi.org/10.1186/2049-1891-5-52, PMID: 25478164

Liao Y, Wang J, Jaehnig EJ, Shi Z, Zhang B. 2019. WebGestalt 2019: gene set analysis toolkit with revamped UIs and APIs. *Nucleic Acids Research* **47**:W199–W205. DOI: https://doi.org/10.1093/nar/gkz401, PMID: 31114916

Lim H, Dey SK, Das SK. 1997. Differential expression of the erbB2 gene in the periimplantation mouse uterus: potential mediator of signaling by epidermal growth factor-like growth factors. *Endocrinology* **138**:1328–1337. DOI: https://doi.org/10.1210/endo.138.3.4991, PMID: 9048643

Lima PD, Zhang J, Dunk C, Lye SJ, Croy BA. 2014. Leukocyte driven-decidual angiogenesis in early pregnancy. *Cellular & Molecular Immunology* **11**:522–537. DOI: https://doi.org/10.1038/cmi.2014.63, PMID: 25066422

Lindström TM, Bennett PR. 2005. The role of nuclear factor kappa B in human labour. *Reproduction* **130**:569–581. DOI: https://doi.org/10.1530/rep.1.00197, PMID: 16264088

Love MI, Huber W, Anders S. 2014. Moderated estimation of fold change and dispersion for RNA-seq data with DESeq2. *Genome Biology* **15**:550. DOI: https://doi.org/10.1186/s13059-014-0550-8, PMID: 25516281

Lu CX, Gong HR, Liu XY, Wang J, Zhao CM, Huang RT, Xue S, Yang YQ. 2016. A novel HAND2 loss-of-function mutation responsible for tetralogy of fallot. *International Journal of Molecular Medicine* **37**:445–451. DOI: https://doi.org/10.3892/ijmm.2015.2436, PMID: 26676105

Lucas ES, Vrljicak P, Muter J, Diniz-da-Costa MM, Brighton PJ, Kong CS, Lipecki J, Fishwick KJ, Odendaal J, Ewington LJ, Quenby S, Ott S, Brosens JJ. 2020. Recurrent pregnancy loss is associated with a pro-senescent decidual response during the peri-implantation window. *Communications Biology* **3**:37. DOI: https://doi.org/10.1038/s42003-020-0763-1, PMID: 31965050

Lynch VJ, Brayer K, Gellersen B, Wagner GP. 2009. HoxA-11 and FOXO1A cooperate to regulate decidual prolactin expression: towards inferring the core transcriptional regulators of decidual genes. *PLOS ONE* **4**:e6845. DOI: https://doi.org/10.1371/journal.pone.0006845, PMID: 19727442

Lynch VJ, Nnamani MC, Kapusta A, Brayer K, Plaza SL, Mazur EC, Emera D, Sheikh SZ, Grützner F, Bauersachs S, Graf A, Young SL, Lieb JD, DeMayo FJ, Feschotte C, Wagner GP. 2015. Ancient transposable elements transformed the uterine regulatory landscape and transcriptome during the evolution of mammalian pregnancy. *Cell Reports* **10**:551–561. DOI: https://doi.org/10.1016/j.celrep.2014.12.052, PMID: 25640180

Maddison WP, Maddison DR. 2019. *Mesquite: A Modular System for Evolutionary Analysis*. http://www.mesquiteproject.org

Marinić M, Rana S, Lynch VJ. 2020. Derivation of endometrial gland organoids from term placenta. *Placenta* **101**:75–79. DOI: https://doi.org/10.1016/j.placenta.2020.08.017, PMID: 32937244

McConaha ME, Eckstrum K, An J, Steinle JJ, Bany BM. 2011. Microarray assessment of the influence of the conceptus on gene expression in the mouse uterus during decidualization. *Reproduction* **141**:511–527. DOI: https://doi.org/10.1530/REP-10-0358, PMID: 21300692

Means AR, Woo S, Harris SE, O'Malley BW. 1975. Estrogen induction of ovalbumin mRNA: evidence for transcription control. *Molecular and Cellular Biochemistry* **7**:33–42. DOI: https://doi.org/10.1007/BF01732161, PMID: 1094273

Menon R, Bonney EA, Condon J, Mesiano S, Taylor RN. 2016. Novel concepts on pregnancy clocks and alarms: redundancy and synergy in human parturition. *Human Reproduction Update* **22**:535–560. DOI: https://doi.org/10.1093/humupd/dmw022, PMID: 27363410

Mesiano S, Chan EC, Fitter JT, Kwek K, Yeo G, Smith R. 2002. Progesterone withdrawal and estrogen activation in human parturition are coordinated by progesterone receptor A expression in the myometrium. *The Journal of Clinical Endocrinology & Metabolism* **87**:2924–2930. DOI: https://doi.org/10.1210/jcem.87.6.8609, PMID: 12050275

Mestre-Citrinovitz AC, Kleff V, Vallejo G, Winterhager E, Saragüeta P. 2015. A suppressive antagonism evidences progesterone and estrogen receptor pathway interaction with concomitant regulation of Hand2,

Bmp2 and ERK during early decidualization. *PLOS ONE* **10**:e0124756. DOI: https://doi.org/10.1371/journal.pone.0124756, PMID: 25897495

Moffett A, Regan L, Braude P. 2004. Natural killer cells, miscarriage, and infertility. *BMJ* **329**:1283–1285. DOI: https://doi.org/10.1136/bmj.329.7477.1283, PMID: 15564263

Moffett A, Loke YW. 2004. The immunological paradox of pregnancy: a reappraisal. *Placenta* **25**:1–8. DOI: https://doi.org/10.1016/S0143-4004(03)00167-X, PMID: 15013633

Moffett-King A. 2002. Natural killer cells and pregnancy. *Nature Reviews Immunology* **2**:656–663. DOI: https://doi.org/10.1038/nri886, PMID: 12209134

Munn DH, Zhou M, Attwood JT, Bondarev I, Conway SJ, Marshall B, Brown C, Mellor AL. 1998. Prevention of allogeneic fetal rejection by tryptophan catabolism. *Science* **281**:1191–1193. DOI: https://doi.org/10.1126/science.281.5380.1191, PMID: 9712583

Muñoz-Fernández R, De La Mata C, Requena F, Martín F, Fernandez-Rubio P, Llorca T, Ruiz-Magaña MJ, Ruiz-Ruiz C, Olivares EG. 2019. Human predecidual stromal cells are mesenchymal stromal/stem cells and have a therapeutic effect in an immune-based mouse model of recurrent spontaneous abortion. *Stem Cell Research & Therapy* **10**:177. DOI: https://doi.org/10.1186/s13287-019-1284-z, PMID: 31200769

Murata H, Tsuzuki T, Kido T, Kakita-Kobayashi M, Kida N, Hisamatsu Y, Okada H. 2019. Progestin-induced heart and neural crest derivatives-expressed transcript 2 inhibits angiopoietin 2 via fibroblast growth factor 9 in human endometrial stromal cells. *Reproductive Biology* **19**:14–21. DOI: https://doi.org/10.1016/j.repbio.2019.02.005, PMID: 30852242

Murata H, Tanaka S, Tsuzuki-Nakao T, Kido T, Kakita-Kobayashi M, Kida N, Hisamatsu Y, Tsubokura H, Hashimoto Y, Kitada M, Okada H. 2020. The transcription factor HAND2 up-regulates transcription of the *IL15* gene in human endometrial stromal cells. *Journal of Biological Chemistry* **295**:9596–9605. DOI: https://doi.org/10.1074/jbc.RA120.012753, PMID: 32444497

Murphy SP, Fast LD, Hanna NN, Sharma S. 2005. Uterine NK cells mediate inflammation-induced fetal demise in IL-10-null mice. *The Journal of Immunology* **175**:4084–4090. DOI: https://doi.org/10.4049/jimmunol.175.6.4084, PMID: 16148158

Murphy SP, Hanna NN, Fast LD, Shaw SK, Berg G, Padbury JF, Romero R, Sharma S. 2009. Evidence for participation of uterine natural killer cells in the mechanisms responsible for spontaneous preterm labor and delivery. *American Journal of Obstetrics and Gynecology* **200**:308.e1–30308. DOI: https://doi.org/10.1016/j.ajog.2008.10.043

Ni N, Li Q. 2017. Tgfβ superfamily signaling and uterine decidualization. *Reproductive Biology and Endocrinology* **15**:0303. DOI: https://doi.org/10.1186/s12958-017-0303-0

Norwitz ER, Bonney EA, Snegovskikh VV, Williams MA, Phillippe M, Park JS, Abrahams VM. 2015. Molecular regulation of parturition: the role of the decidual clock. *Cold Spring Harbor Perspectives in Medicine* **5**:a023143. DOI: https://doi.org/10.1101/cshperspect.a023143, PMID: 25918180

Okada S, Okada H, Sanezumi M, Nakajima T, Yasuda K, Kanzaki H. 2000. Expression of interleukin-15 in human endometrium and decidua. *Molecular Human Reproduction* **6**:75–80. DOI: https://doi.org/10.1093/molehr/6.1.75, PMID: 10611264

Okada H, Nakajima T, Yasuda K, Kanzaki H. 2004. Interleukin-1 inhibits interleukin-15 production by progesterone during in vitro decidualization in human. *Journal of Reproductive Immunology* **61**:3–12. DOI: https://doi.org/10.1016/j.jri.2003.10.002, PMID: 14967219

Olcese J. 2012. Circadian aspects of mammalian parturition: a review. *Molecular and Cellular Endocrinology* **349**:62–67. DOI: https://doi.org/10.1016/j.mce.2011.06.041, PMID: 21777654

Olcese J, Lozier S, Paradise C. 2013. Melatonin and the circadian timing of human parturition. *Reproductive Sciences* **20**:168–174. DOI: https://doi.org/10.1177/1933719112442244, PMID: 22556015

Oliver EA, Buhimschi CS, Dulay AT, Baumbusch MA, Abdel-Razeq SS, Lee SY, Zhao G, Jing S, Pettker CM, Buhimschi IA. 2011. Activation of the receptor for advanced glycation end products system in women with severe preeclampsia. *The Journal of Clinical Endocrinology & Metabolism* **96**:689–698. DOI: https://doi.org/10.1210/jc.2010-1418, PMID: 21325454

Osman I, Young A, Ledingham MA, Thomson AJ, Jordan F, Greer IA, Norman JE. 2003. Leukocyte density and pro-inflammatory cytokine expression in human fetal membranes, decidua, cervix and myometrium before and during labour at term. *Molecular Human Reproduction* **9**:41–45. DOI: https://doi.org/10.1093/molehr/gag001, PMID: 12529419

O'Mara TA, Spurdle AB, Glubb DM, Endometrial Cancer Association Consortium Endometrial Cancer Association Consortium. 2019. Analysis of promoter-associated chromatin interactions reveals biologically relevant candidate target genes at endometrial cancer risk loci. *Cancers* **11**:1440. DOI: https://doi.org/10.3390/cancers11101440

Paiva P, Salamonsen LA, Manuelpillai U, Dimitriadis E. 2009. Interleukin 11 inhibits human trophoblast invasion indicating a likely role in the decidual restraint of trophoblast invasion during placentation. *Biology of Reproduction* **80**:302–310. DOI: https://doi.org/10.1095/biolreprod.108.071415, PMID: 18987331

Peng S, Li J, Miao C, Jia L, Hu Z, Zhao P, Li J, Zhang Y, Chen Q, Duan E. 2008. Dickkopf-1 secreted by decidual cells promotes trophoblast cell invasion during murine placentation. *Reproduction* **135**:367–375. DOI: https://doi.org/10.1530/REP-07-0191, PMID: 18299430

Pepe GJ, Albrecht ED. 1995. 'Actions of placental and fetal adrenal steroid hormones in primate pregnancy'. *Endocrine Reviews* **16**:608–648. DOI: https://doi.org/10.1210/edrv-16-5-608, PMID: 8529574

Pertea M, Pertea GM, Antonescu CM, Chang TC, Mendell JT, Salzberg SL. 2015. StringTie enables improved reconstruction of a transcriptome from RNA-seq reads. *Nature Biotechnology* **33**:290–295. DOI: https://doi.org/10.1038/nbt.3122, PMID: 25690850

Pertea M, Kim D, Pertea GM, Leek JT, Salzberg SL. 2016. Transcript-level expression analysis of RNA-seq experiments with HISAT, StringTie and Ballgown. *Nature Protocols* **11**:1650–1667. DOI: https://doi.org/10.1038/nprot.2016.095, PMID: 27560171

Peters GA, Yi L, Skomorovska-Prokvolit Y, Patel B, Amini P, Tan H, Mesiano S. 2016. Inflammatory stimuli increase progesterone receptor-A stability and transrepressive activity in myometrial cells. *Endocrinology* **158**: en.2016-1537. DOI: https://doi.org/10.1210/en.2016-1537

Pinto RM, Lerner U, Glauberman M, Pontelli H. 1966. Influence of estradiol-17-beta upon the oxytocic action of oxytocin in the pregnant human uterus. *American Journal of Obstetrics and Gynecology* **96**:857–862. DOI: https://doi.org/10.1016/0002-9378(66)90682-X, PMID: 5927295

Plunkett J, Doniger S, Orabona G, Morgan T, Haataja R, Hallman M, Puttonen H, Menon R, Kuczynski E, Norwitz E, Snegovskikh V, Palotie A, Peltonen L, Fellman V, DeFranco EA, Chaudhari BP, McGregor TL, McElroy JJ, Oetjens MT, Teramo K, et al. 2011. An evolutionary genomic approach to identify genes involved in human birth timing. *PLOS Genetics* **7**:e1001365. DOI: https://doi.org/10.1371/journal.pgen.1001365, PMID: 21533219

Ratajczak CK, Fay JC, Muglia LJ. 2010. Preventing preterm birth: the past limitations and new potential of animal models. *Disease Models & Mechanisms* **3**:407–414. DOI: https://doi.org/10.1242/dmm.001701, PMID: 20610693

Renaud SJ, Scott RL, Chakraborty D, Rumi MA, Soares MJ. 2017. Natural killer-cell deficiency alters placental development in rats. *Biology of Reproduction* **96**:145–158. DOI: https://doi.org/10.1095/biolreprod.116.142752, PMID: 28395334

Renfree MB. 2010. Review: marsupials: placental mammals with a difference. *Placenta* **31 Suppl**:S21–S26. DOI: https://doi.org/10.1016/j.placenta.2009.12.023, PMID: 20079531

Renfree MB, Blanden DR. 2000. Progesterone and oestrogen receptors in the female genital tract throughout pregnancy in tammar wallabies. *Reproduction* **119**:121–128. DOI: https://doi.org/10.1530/jrf.0.1190121, PMID: 10864821

Renfree M, Shaw G. 2001. *Reproduction in Monotremes and Marsupials*. In: Renfree M (Ed). *Encyclopedia of Life Sciences*. Chichester, UK: John Wiley & Sons, Ltd. p. 1–10. DOI: https://doi.org/10.1038/npg.els.0001856

Richards RG, Brar AK, Frank GR, Hartman SM, Jikihara H. 1995. Fibroblast cells from term human decidua closely resemble endometrial stromal cells: induction of prolactin and insulin-like growth factor binding protein-1 expression. *Biology of Reproduction* **52**:609–615. DOI: https://doi.org/10.1095/biolreprod52.3.609, PMID: 7756454

Rinaldi SF, Hutchinson JL, Rossi AG, Norman JE. 2011. Anti-inflammatory mediators as physiological and pharmacological regulators of parturition. *Expert Review of Clinical Immunology* **7**:675–696. DOI: https://doi.org/10.1586/eci.11.58, PMID: 21895479

Rinaldi SF, Rossi AG, Saunders PTK, Norman JE. 2015. Immune cells and preterm labour: do invariant NKT cells hold the key? *Molecular Human Reproduction* **21**:309–312. DOI: https://doi.org/10.1093/molehr/gav002, PMID: 25589516

Rinehart CA, Lyn-Cook BD, Kaufman DG. 1988. Gland formation from human endometrial epithelial cells in vitro. *In Vitro Cellular & Developmental Biology* **24**:1037–1041. DOI: https://doi.org/10.1007/BF02620878, PMID: 3182555

Robson A, Harris LK, Innes BA, Lash GE, Aljunaidy MM, Aplin JD, Baker PN, Robson SC, Bulmer JN. 2012. Uterine natural killer cells initiate spiral artery remodeling in human pregnancy. *The FASEB Journal* **26**:4876–4885. DOI: https://doi.org/10.1096/fj.12-210310, PMID: 22919072

Roizen J, Luedke CE, Herzog ED, Muglia LJ. 2007. Oxytocin in the circadian timing of birth. *PLOS ONE* **2**:e922. DOI: https://doi.org/10.1371/journal.pone.0000922, PMID: 17895964

Sakabe NJ, Aneas I, Knoblauch N, Sobreira DR, Clark N, Paz C, Horth C, Ziffra R, Kaur H, Liu X, Anderson R, Morrison J, Cheung VC, Grotegut C, Reddy TE, Jacobsson B, Hallman M, Teramo K, Murtha A, Kessler J, et al. 2020. Transcriptome and regulatory maps of decidua-derived stromal cells inform gene discovery in preterm birth. *Science Advances* **6**:eabc8696. DOI: https://doi.org/10.1126/sciadv.abc8696, PMID: 33268355

Shen L, Li XF, Shen AD, Wang Q, Liu CX, Guo YJ, Song ZJ, Li ZZ. 2010. Transcription factor HAND2 mutations in sporadic Chinese patients with congenital heart disease. *Chinese Medical Journal* **123**:1623–1627. DOI: https://doi.org/10.3760/cma.j.issn.0366-6999.2010.13.002, PMID: 20819618

Shindoh H, Okada H, Tsuzuki T, Nishigaki A, Kanzaki H. 2014. Requirement of heart and neural crest derivatives-expressed transcript 2 during decidualization of human endometrial stromal cells in vitro. *Fertility and Sterility* **101**:1781–1790. DOI: https://doi.org/10.1016/j.fertnstert.2014.03.013, PMID: 24745730

Shynlova O, Nedd-Roderique T, Li Y, Dorogin A, Lye SJ. 2013. Myometrial immune cells contribute to term parturition, preterm labour and post-partum involution in mice. *Journal of Cellular and Molecular Medicine* **17**:90–102. DOI: https://doi.org/10.1111/j.1582-4934.2012.01650.x, PMID: 23205502

Smith R, Smith JI, Shen X, Engel PJ, Bowman ME, McGrath SA, Bisits AM, McElduff P, Giles WB, Smith DW. 2009a. Patterns of plasma corticotropin-releasing hormone, progesterone, estradiol, and estriol change and the onset of human labor. *The Journal of Clinical Endocrinology & Metabolism* **94**:2066–2074. DOI: https://doi.org/10.1210/jc.2008-2257, PMID: 19258402

Smith SD, Dunk CE, Aplin JD, Harris LK, Jones RL. 2009b. Evidence for immune cell involvement in decidual spiral arteriole remodeling in early human pregnancy. *The American Journal of Pathology* **174**:1959–1971. DOI: https://doi.org/10.2353/ajpath.2009.080995, PMID: 19349361

Smyth GK, Ritchie M, Thorne N, Wettenhall J, Shi W, Hu Y. 2002. *Limma: Linear Models for Microarray and RNA-Seq Data User's Guide*. bioconductor. https://bioconductor.org/packages/release/bioc/vignettes/limma/inst/doc/usersguide.pdf

Sonderegger S, Pollheimer J, Knöfler M. 2010. Wnt signalling in implantation, decidualisation and placental differentiation–review. *Placenta* **31**:839–847. DOI: https://doi.org/10.1016/j.placenta.2010.07.011, PMID: 20716463

Srivastava D, Thomas T, Lin Q, Kirby ML, Brown D, Olson EN. 1997. Regulation of cardiac mesodermal and neural crest development by the bHLH transcription factor, dHAND. *Nature Genetics* **16**:154–160. DOI: https://doi.org/10.1038/ng0697-154, PMID: 9171826

Šućurović S, Nikolić T, Brosens JJ, Mulac-Jeričević B. 2020. Analysis of heart and neural crest derivatives-expressed protein 2 (HAND2)-progesterone interactions in peri-implantation endometrium†. *Biology of Reproduction* **102**:1111–1121. DOI: https://doi.org/10.1093/biolre/ioaa013, PMID: 31982918

Sun Y-M, Wang J, Qiu X-B, Yuan F, Li R-G, Xu Y-J, Qu X-K, Shi H-Y, Hou X-M, Huang R-T, Xue S, Yang Y-Q. 2016. A HAND2 loss-of-function mutation causes familial ventricular septal defect and pulmonary stenosis. *G3 Genes|Genomes|Genetics* **6**:987–992.

Suryawanshi H, Morozov P, Straus A, Sahasrabudhe N, Max KEA, Garzia A, Kustagi M, Tuschl T, Williams Z. 2018. A single-cell survey of the human first-trimester placenta and decidua. *Science Advances* **4**:eaau4788. DOI: https://doi.org/10.1126/sciadv.aau4788, PMID: 30402542

Swaggart KA, Pavlicev M, Muglia LJ. 2015. Genomics of preterm birth. *Cold Spring Harbor Perspectives in Medicine* **5**:a023127. DOI: https://doi.org/10.1101/cshperspect.a023127, PMID: 25646385

Tabanelli S, Tang B, Gurpide E. 1992. In vitro decidualization of human endometrial stromal cells. *The Journal of Steroid Biochemistry and Molecular Biology* **42**:337–344. DOI: https://doi.org/10.1016/0960-0760(92)90137-8

Talbi S, Hamilton AE, Vo KC, Tulac S, Overgaard MT, Dosiou C, Le Shay N, Nezhat CN, Kempson R, Lessey BA, Nayak NR, Giudice LC. 2006. Molecular phenotyping of human endometrium distinguishes menstrual cycle phases and underlying biological processes in normo-ovulatory women. *Endocrinology* **147**:1097–1121. DOI: https://doi.org/10.1210/en.2005-1076, PMID: 16306079

Tamura M, Hosoya M, Fujita M, Iida T, Amano T, Maeno A, Kataoka T, Otsuka T, Tanaka S, Tomizawa S, Shiroishi T. 2013. Overdosage of Hand2 causes limb and heart defects in the human chromosomal disorder partial trisomy distal 4q. *Human Molecular Genetics* **22**:2471–2481. DOI: https://doi.org/10.1093/hmg/ddt099, PMID: 23449628

Thomson AJ, Telfer JF, Young A, Campbell S, Stewart CJ, Cameron IT, Greer IA, Norman JE. 1999. Leukocytes infiltrate the myometrium during human parturition: further evidence that labour is an inflammatory process. *Human Reproduction* **14**:229–236. DOI: https://doi.org/10.1093/humrep/14.1.229, PMID: 10374126

Turco MY, Gardner L, Hughes J, Cindrova-Davies T, Gomez MJ, Farrell L, Hollinshead M, Marsh SGE, Brosens JJ, Critchley HO, Simons BD, Hemberger M, Koo BK, Moffett A, Burton GJ. 2017. Long-term, hormone-responsive organoid cultures of human endometrium in a chemically defined medium. *Nature Cell Biology* **19**:568–577. DOI: https://doi.org/10.1038/ncb3516, PMID: 28394884

Turco MY, Gardner L, Kay RG, Hamilton RS, Prater M, Hollinshead MS, McWhinnie A, Esposito L, Fernando R, Skelton H, Reimann F, Gribble FM, Sharkey A, Marsh SGE, O'Rahilly S, Hemberger M, Burton GJ, Moffett A. 2018. Trophoblast organoids as a model for maternal-fetal interactions during human placentation. *Nature* **564**:263–267. DOI: https://doi.org/10.1038/s41586-018-0753-3, PMID: 30487605

Uhlén M, Fagerberg L, Hallström BM, Lindskog C, Oksvold P, Mardinoglu A, Sivertsson Å, Kampf C, Sjöstedt E, Asplund A, Olsson I, Edlund K, Lundberg E, Navani S, Szigyarto CA, Odeberg J, Djureinovic D, Takanen JO, Hober S, Alm T, et al. 2015. Tissue-based map of the human proteome. *Science* **347**:1260419. DOI: https://doi.org/10.1126/science.1260419, PMID: 25613900

Varas Enriquez PJ, McKerracher LJ, Elliot MG. 2018. Pre-eclampsia and maternal-fetal conflict. *Evolution, Medicine, and Public Health* **2018**:217–218. DOI: https://doi.org/10.1093/emph/eoy029, PMID: 30374404

Varki N, Anderson D, Herndon JG, Pham T, Gregg CJ, Cheriyan M, Murphy J, Strobert E, Fritz J, Else JG, Varki A. 2009. Heart disease is common in humans and chimpanzees, but is caused by different pathological processes. *Evolutionary Applications* **2**:101–112. DOI: https://doi.org/10.1111/j.1752-4571.2008.00064.x, PMID: 25567850

Varki A. 2012. Nothing in medicine makes sense, except in the light of evolution. *Journal of Molecular Medicine* **90**:481–494. DOI: https://doi.org/10.1007/s00109-012-0900-5, PMID: 22538272

Varki NM, Varki A. 2015. On the apparent rarity of epithelial cancers in captive chimpanzees. *Philosophical Transactions of the Royal Society B: Biological Sciences* **370**:20140225. DOI: https://doi.org/10.1098/rstb.2014.0225

Vento-Tormo R, Efremova M, Botting RA, Turco MY, Vento-Tormo M, Meyer KB, Park JE, Stephenson E, Polański K, Goncalves A, Gardner L, Holmqvist S, Henriksson J, Zou A, Sharkey AM, Millar B, Innes B, Wood L, Wilbrey-Clark A, Payne RP, et al. 2018. Single-cell reconstruction of the early maternal-fetal interface in humans. *Nature* **563**:347–353. DOI: https://doi.org/10.1038/s41586-018-0698-6, PMID: 30429548

Verma S, Hiby SE, Loke YW, King A. 2000. Human decidual natural killer cells express the receptor for and respond to the cytokine interleukin 15. *Biology of Reproduction* **62**:959–968. DOI: https://doi.org/10.1095/biolreprod62.4.959, PMID: 10727265

Wagner GP, Kin K, Lynch VJ. 2012. Measurement of mRNA abundance using RNA-seq data: RPKM measure is inconsistent among samples. *Theory in Biosciences* **131**:281–285. DOI: https://doi.org/10.1007/s12064-012-0162-3, PMID: 22872506

Wagner GP, Kin K, Lynch VJ. 2013. A model based criterion for gene expression calls using RNA-seq data. *Theory in Biosciences* **132**:159–164. DOI: https://doi.org/10.1007/s12064-013-0178-3, PMID: 23615947

Wallace AE, Host AJ, Whitley GS, Cartwright JE. 2013. Decidual natural killer cell interactions with trophoblasts are impaired in pregnancies at increased risk of preeclampsia. *The American Journal of Pathology* **183**:1853–1861. DOI: https://doi.org/10.1016/j.ajpath.2013.08.023

Wallace AE, Fraser R, Gurung S, Goulwara SS, Whitley GS, Johnstone AP, Cartwright JE. 2014. Increased angiogenic factor secretion by decidual natural killer cells from pregnancies with high uterine artery resistance alters trophoblast function. *Human Reproduction* **29**:652–660. DOI: https://doi.org/10.1093/humrep/deu017, PMID: 24522839

Wang Q, Lu J, Zhang S, Wang S, Wang W, Wang B, Wang F, Chen Q, Duan E, Leitges M, Kispert A, Wang H. 2013. Wnt6 is essential for stromal cell proliferation during decidualization in Mice1. *Biology of Reproduction* **88**:104687. DOI: https://doi.org/10.1095/biolreprod.112.104687

Warrington NM, Beaumont RN, Horikoshi M, Day FR, Helgeland Ø, Laurin C, Bacelis J, Peng S, Hao K, Feenstra B, Wood AR, Mahajan A, Tyrrell J, Robertson NR, Rayner NW, Qiao Z, Moen GH, Vaudel M, Marsit CJ, Chen J, et al. 2019. Maternal and fetal genetic effects on birth weight and their relevance to cardio-metabolic risk factors. *Nature Genetics* **51**:804–814. DOI: https://doi.org/10.1038/s41588-019-0403-1, PMID: 31043758

Welsh T, Johnson M, Yi L, Tan H, Rahman R, Merlino A, Zakar T, Mesiano S. 2012. Estrogen receptor (ER) expression and function in the pregnant human myometrium: estradiol via erα activates ERK1/2 signaling in term myometrium. *Journal of Endocrinology* **212**:227–238. DOI: https://doi.org/10.1530/JOE-11-0358

Wetendorf M, DeMayo FJ. 2012. The progesterone receptor regulates implantation, decidualization, and glandular development via a complex paracrine signaling network. *Molecular and Cellular Endocrinology* **357**:108–118. DOI: https://doi.org/10.1016/j.mce.2011.10.028, PMID: 22115959

Williams PJ, Searle RF, Robson SC, Innes BA, Bulmer JN. 2009. Decidual leucocyte populations in early to late gestation normal human pregnancy. *Journal of Reproductive Immunology* **82**:24–31. DOI: https://doi.org/10.1016/j.jri.2009.08.001, PMID: 19732959

Wilson RA, Mesiano SA. 2020. Progesterone signaling in myometrial cells: role in human pregnancy and parturition. *Current Opinion in Physiology* **13**:117–122. DOI: https://doi.org/10.1016/j.cophys.2019.09.007

Winn VD, Haimov-Kochman R, Paquet AC, Yang YJ, Madhusudhan MS, Gormley M, Feng KT, Bernlohr DA, McDonagh S, Pereira L, Sali A, Fisher SJ. 2007. Gene expression profiling of the human maternal-fetal interface reveals dramatic changes between midgestation and term. *Endocrinology* **148**:1059–1079. DOI: https://doi.org/10.1210/en.2006-0683, PMID: 17170095

Ying Y, Zhao GQ. 2000. Detection of multiple bone morphogenetic protein messenger ribonucleic acids and their signal transducer, Smad1, during mouse decidualization. *Biology of Reproduction* **63**:1781–1786. DOI: https://doi.org/10.1095/biolreprod63.6.1781, PMID: 11090449

Young A, Thomson AJ, Ledingham M, Jordan F, Greer IA, Norman JE. 2002. Immunolocalization of proinflammatory cytokines in myometrium, cervix, and fetal membranes during human parturition at term. *Biology of Reproduction* **66**:445–449. DOI: https://doi.org/10.1095/biolreprod66.2.445, PMID: 11804961

Young CE, McDonald IR. 1982. Oestrogen receptors in the genital tract of the Australian marsupial *Trichosurus vulpecula*. *General and Comparative Endocrinology* **46**:417–427. DOI: https://doi.org/10.1016/0016-6480(82)90095-8, PMID: 7095404

Zhang Y, Liu T, Meyer CA, Eeckhoute J, Johnson DS, Bernstein BE, Nussbaum C, Myers RM, Brown M, Li W, Liu XS. 2008. Model-based analysis of ChIP-Seq (MACS). *Genome Biology* **9**:R137. DOI: https://doi.org/10.1186/gb-2008-9-9-r137

Zhang J, Dunk CE, Lye SJ. 2013. Sphingosine signalling regulates decidual NK cell angiogenic phenotype and trophoblast migration. *Human Reproduction* **28**:3026–3037. DOI: https://doi.org/10.1093/humrep/det339, PMID: 24001716

Zhu XM, Han T, Sargent IL, Wang YL, Yao YQ. 2009. Conditioned medium from human decidual stromal cells has a concentration-dependent effect on trophoblast cell invasion. *Placenta* **30**:74–78. DOI: https://doi.org/10.1016/j.placenta.2008.09.013, PMID: 19007982

Zygmunt M, Hahn D, Kiesenbauer N, Münstedt K, Lang U. 1998. Invasion of cytotrophoblastic (JEG-3) cells is up-regulated by interleukin-15 in vitro. *American Journal of Reproductive Immunology* **40**:326–331. DOI: https://doi.org/10.1111/j.1600-0897.1998.tb00061.x, PMID: 9870075